# Differences Among Genotypes and Phenotypic Plasticity Determine Intraspecific Variability in Cell Size, Cellular Nutrients, and Stoichiometry in the Diatom *Chaetoceros affinis*

Master's Thesis

In Marine Environmental Science


Submitted by: Julia Romberg (5351807)

First examiner: Dr. rer. nat. Birte Matthiessen

Second examiner: Dr. rer. nat. Stefanie Moorthi


Oldenburg, October 2022

GEOMAR
Helmholtz-Zentrum für Ozeanforschung Kiel

# Table of contents

# List of figures

# List of figures in Appendix

# List of tables



# List of tables in Appendix



# List of abbreviations

| | |
|---|---|
| POC | Particulate organic carbon |
| PON | Particulate organic nitrogen |
| C | Carbon |
| N | Nitrogen |
| P | Phosphorus |
| Si | Silicate |
| N:P | Nitrogen-to-phosphorus ratio |
| C:N | Carbon-to-nitrogen ratio |
| N treatment | Nitrate treatment |
| G | Genotype identity |

# Abstract

Intraspecific trait variability originates from variability among genotypes and intragenotypic plasticity, which are both shown to be attributed as important and can be of the same magnitude as or even exceed interspecific variability. To better understand the aspects of phytoplankton intraspecific trait variability, the among-genotype and plasticity-driven variability of cell size, cellular carbon (POC), and nitrogen (PON), stoichiometry and their interrelations were investigated using the diatom *Chaetoceros affinis* as representative of the ecologically and functionally important group. An experimental set-up was designed in a full-factorial manner, in which nine genotypes of *C. affinis* were individually treated with a nutrient gradient spanning seven different nitrate concentrations while phosphate was held constant, covering strong nitrate-limited to Redfield conditions (16 N:1P) in the medium. Cell size, cellular nutrient content, and stoichiometry were assessed after seven days of growth at the end of the experiment. I hypothesized to find (i) intraspecific variability in cell size, cellular nutrients, and stoichiometry in response to the applied nitrate gradient, which (ii) can be attributed to both plasticity and differences among genotypes. Furthermore, I conjectured (iii) that cell size may be a determinant for both plastic and intergenotypic variations in cellular nutrient content and stoichiometry. Precisely, I expected cell size to increase with nitrate supply while POC, PON, and stoichiometry would decrease. Across all genotypes, cellular POC and PON showed U-shaped responses, whereas a hump-shaped response of cell size and carbon-to-nitrogen ratio (C:N) to increasing nitrate concentrations was found. Additionally, intraspecific variability was identified in cell size and C:N in the form of the reaction norms on both the plasticity level, indicated by significantly different reaction norms within single genotypes, and among genotypes in response to the applied nitrate gradient. As cell size positively correlated with C:N across and within genotypes, my results suggest that cell size plays a role in explaining the unexpected unimodal stoichiometric response to nutrients. The relationship between increasing cell size and increasing C:N ratio could be explained by the fact that smaller cells contain a higher relative abundance of nitrogen-rich molecules such as nucleic acids and membrane proteins, while they store fewer carbon-rich compounds such as lipids and carbohydrates. Larger cells, however, have higher storage capacities such as vacuoles in

which mainly carbon is stored. This may therefore explain why larger cells have a higher C:N ratio compared to smaller cells.

Two factors, the successional stage and potential phosphate-limitation, that may have confounded the conclusions of this study are discussed and ways to control for them are suggested. Even though these two factors could have additionally affected the results, a subset of the data on which these factors had no influence supported the role of cell size in explaining differences in stoichiometry (C:N). These differences, however, seemed to be driven by different elements on different levels, within and across genotypes. My data underpin the importance to consider the different levels from which the sources of intraspecific trait variability can arise, to ultimately understand the drivers and consequences of intraspecific variation in functionally important groups, such as diatoms. In conclusion, the investigation of intraspecific trait variability remains important and should be considered context-specific. This may ultimately help to assess the capability of phytoplankton groups to cope with climate change and to model the consequences of changes for higher trophic levels or the biological carbon pump.

Keywords: intraspecific trait variability, variability among genotypes, phenotypic plasticity, phytoplankton, cell size, stoichiometry, *Chaetoceros affinis*, diatom, nutrient

# 1|Introduction

Phytoplankton as microbial primary producers provide the basis of marine and freshwater food webs, contribute half to the world's primary productivity, and drive global biogeochemical cycles (Falkowski *et al.* 1998; Field *et al.* 1998). Among the different groups of marine phytoplankton, diatoms are an important part, that evolved in the early Mesozoic (~190-250 million years ago) (Kooistra & Medlin 1996; Benoiston *et al.* 2017) and are characterized by the unique feature of silicified cell walls. Diatoms are distributed in almost all aquatic habitats and are particularly associated with nutrient-rich conditions that can be found in coastal temperate waters or upwelling areas. Moreover, they are the dominant taxa during seasonal blooms, such as the North Atlantic spring bloom (Malviya *et al.* 2016; Armbrust 2009; Cervato & Burckle 2003; Bopp *et al.* 2005; Rynearson *et al.* 2013). Diatoms account for up to 40% of marine primary productivity (Tréguer *et al.* 1995; Tréguer *et al.* 2018) and are therefore considered key players in the global oxygen production, trophic transfer to higher levels in the food web, and carbon transport into the ocean.

## Role of cell size in plankton ecology

Nutrient availability, among other environmental factors such as temperature or grazing pressure, regulates phytoplankton biomass production, community composition, and importantly size structure (Irwin *et al.* 2006; Marañón 2015; Peter & Sommer 2013). Phytoplankton size, including colonies, spans up to nine orders of magnitude from the smallest cyanobacteria (<0.1 $\mu m^3$) to the largest diatoms (>$10^8$ $\mu m^3$) (Finkel *et al.* 2010; Marañón 2015). Cell size is considered a master trait in phytoplankton ecology (Litchman *et al.* 2010), as it is one of the most fundamental traits, affecting almost all aspects, such as physiological, demographic, behavioural, and predation-related traits (Peters 1993) from the cellular, population and ultimately up to the community level (Raven 1998; Chisholm 1992; Litchman & Klausmeier 2008; Litchman *et al.* 2009; Peters 1993; Brown *et al.* 1993). Examples of traits and related process rates that are influenced by, or correlated with cell size are growth rate, photosynthesis, and respiration (Finkel & Irwin 2000; Tang 1995; Tang & Peters 1995), as well as sinking and grazing rates (Kiørboe 1993) nutrient diffusion, uptake, and requirements (Pasciak & Gavis 1974; Aksnes & Egge 1991; Litchman *et al.* 2007). Previous studies found that the occurrence of smaller cells is

associated with low concentrations of available nutrients, while that of larger cells tends to be associated with replete nutrient conditions (Irwin *et al.* 2006; Winder *et al.* 2009; Finkel *et al.* 2010; Marañón 2015; Hillebrand *et al.* 2022). The reason for this is that small phytoplankton cells due to higher surface-to-volume ratios show higher affinity for nutrients and lower diffusion limitation (Aksnes & Egge 1991; Hein *et al.* 1995; Edwards *et al.* 2012). Thus, in nutrient-limited conditions, small cells such as picoplankton, coccolithophores, or small nanoflagellates, are competitively superior over larger cells (Lewandowska *et al.* 2014; Litchman *et al.* 2015). Larger cells such as diatoms, for example, are better competitors in nutrient replete and/or pulsed conditions because they are characterised by high uptake and growth rates and storage capacities while showing a lower affinity for nutrients (Sommer 1984; Edwards *et al.* 2012; Marañón 2015; Sommer *et al.* 2016).

Nutrient-regulated phytoplankton size structure ultimately determines food web organisation and complexity and consequently the efficiency of energy transfer towards upper trophic levels or export of organic matter through the biological carbon pump (Litchman *et al.* 2009). This means that if phytoplankton size structure is dominated by smaller cells (<2 µm in diameter), tight trophic coupling between photoautotrophs, heterotrophic bacteria, and their protist predators lead to more trophic levels and results in higher complexities compared to systems based on larger cells (Azam *et al.* 1983; Legendre & Le Fèvre 1995; Marañón 2015).

Besides cell size, resource availability, most notably of the macronutrients, carbon, nitrogen, and phosphorus (Sterner & Elser 2002), also affects cellular nutrients and consequently elemental stoichiometry. On top of these common resources, diatoms additionally require silicate to build silicified cell walls. Elemental stoichiometry provides an important toolkit for understanding relationships between environmental nutrient supply, nutrient uptake, species composition, producer-consumer interactions, and biogeochemical cycling (Schulhof *et al.* 2019). Furthermore, stoichiometry can be an indicator of nutrient stress; the ratio of carbon to a limiting nutrient (Goldman *et al.* (1979) can serve as a proxy for the strength of nutrient limitation. Stoichiometry of phytoplankton cells may vary within and across taxonomic groups and depend on various traits such as growth rate and ultimately size (Finkel *et al.* 2010; Mei *et al.* 2011).

The relationships between cell size and nutrients and consequently cellular stoichiometry can be investigated at different levels of biological organisation. Since the first general insights into intraspecific trait variation in the 1970s, a number of studies have determined the relationship between cell size and nutrients among different species. Intraspecific variability, however, was almost disregarded until the early 2000s (Bolnick *et al.* 2011 and references therein). Climate change and projected changes in this respect have increased the urgency to also understand the drivers and consequences of intraspecific variation in cell size in response to different environmental conditions.

Although several studies on intraspecific variability, especially in cell size, in response to changing environmental conditions have been published in recent years (e.g. Malerba *et al.* 2016), it remains important to understand the magnitude of these responses of functionally important groups such as diatoms in greater detail. This is important in order to better understand, for example, changes in species or population dynamics, which can ultimately influence food web structure (Sommer *et al.* 2002; Peter & Sommer 2015).

## Intraspecific variability in traits

Generally, intraspecific trait variability in phytoplankton ecology is considered important to cope with environmental fluctuations (Bolnick *et al.* 2011; Malerba *et al.* 2016; Orizar & Lewandowska 2022). It has been shown by means of a global meta-analysis for various functional traits and plant communities that intraspecific variability can be of similar magnitude as or even exceed interspecific variability (Siefert *et al.* 2015). For example, intraspecific and interspecific trait variability has been demonstrated to be of similar magnitude in leaf mass per area in the deciduous tree species *Nothofagus pumilio* compared to interspecific variation among northern hemisphere deciduous broad-leaved tree species (Fajardo & Piper 2011). Examples of intraspecific variability even exceeding interspecific variability have also been shown for seed sizes of pitcher plants in the genus *Sarraceniaceae* (Ellison 2001). Several studies suggested the importance of intraspecific variability for community assembly and thus to account for the considerable phenotypic and genotypic variation within and among populations of single species (Violle *et al.* 2012; Des Roches *et al.* 2018).

Also in phytoplankton, intraspecific variability has been demonstrated to be of similar magnitude as or even exceed interspecific variability (Malerba *et al.* 2016). In fact, it has

been shown that mean phytoplankton community cell size changes in response to temperature are due to both inter- and intraspecific shifts (Peter & Sommer 2012). Due to the clonal reproduction mode of phytoplankton, there are two sources from which intraspecific trait variability, and thus potential shifts, can arise. That is first, phenotypic plasticity and second, variability among different genotypes. Phenotypic plasticity is defined as the expression of different phenotypes by one individual or genotype (Bradshaw 1965). Recent studies found significant phenotypic plasticity in several phytoplankton species along different environmental gradients. For example, the stoichiometry of the monoclonal green algae *Clamydomonas reinhardii* was influenced by temperature changes (Thrane *et al.* 2017). Furthermore, genotypes of two coccolithophore species and one diatom species showed phenotypic plasticity in different growth rates, but also a high potential for phenotypic buffering, in response to elevated $CO_2$ conditions (Hattich *et al.* 2017). Interestingly, the variability of plastic responses of ecologically relevant traits, such as growth and cell size, of different pico-phytoplankton *Ostreococcus taurii* ecotypes to increasing seawater $CO_2$ concentration was shown to be similar in magnitude to the variability among phytoplankton species belonging to different functional groups (Schaum *et al.* 2013). Likewise, the plasticity-driven variability of traits related to light use in terrestrial plants was shown to be of equal magnitude to the variability among different species (Valladares *et al.* 2000).

In addition to phenotypic plasticity, intraspecific trait variation may also arise from variability among different genotypes. Different genotypes of a species can but do not necessarily have to differ in their phenotypes. Examples of variability among genotypes were demonstrated in the dinoflagellate *Alexandrium ostenfeldii* and the diatom *Skeletonema marinoi* under different environmental conditions such as salinity, temperature gradients, and $pCO_2$ (Orizar & Lewandowska 2022; Kremp *et al.* 2012; Brandenburg *et al.* 2021). Boyd *et al.* (2013) found variability among genotypes of two *Thalassiosira* species in response to different temperature regimes.

Regarding the above-explained relationship between cell size and nutrients, Malerba *et al.* (2016) showed that cell size variations among and within strains of the phytoplankton species *Desmodesmus armatus* affect nutrient uptake and utilisation-related traits. This points to the importance of a more detailed understanding of intraspecific trait variation and its potential functional consequences.

## Research questions

Because major aspects that relate to nutrient uptake and cellular stoichiometry scale with cell size (Aksnes & Egge 1991; Litchman *et al.* 2007) and the highlighted importance of intraspecific variability in this respect (Malerba *et al.* 2016), I aimed to study how nutrient-driven intraspecific variation in cell size correlates with cellular nutrients and stoichiometry.

The main objectives of this study are to investigate, first, how different nutrient regimes affect phenotypic plasticity and variability among genotypes in intraspecific cell size, cellular nutrient content, and stoichiometry; and second, how these response variables relate to each other. To do so, I formulated the following hypotheses and tested them by manipulating nine different genotypes of the diatom *Chaetoceros affinis* as representatives of the important taxonomic group, with seven different nutrient levels in a full factorial manner.

## Hypotheses

1. Dissolved nutrient availability alters cell size, cellular POC, PON, and stoichiometry, which further depend on genotype identity.
2. Intraspecific variability in cell size, cellular POC, PON, and stoichiometry can be attributed to both phenotypic plasticity, and differences among genotypes.
3. Cell size is a strong determinant for both plastic and intergenotypic variations in cellular POC, PON, and stoichiometry.

# 2|Material and methods

## Experimental design and setup

To test the proposed hypotheses, an experiment was performed at GEOMAR, Kiel, using the diatom *Chaetoceros affinis* (hereafter referred to as *C. affinis*) comprising nine different genotypes. The nine genotypes examined, were isolated in 2014 and 2015 off the coast of Gran Canary, Spain. Prior to the experiment, all genotypes were acclimated for 14 days in 30 µmol $L^{-1}$ nitrogen (N), 1.8 µmol $L^{-1}$ phosphorus (P), and 40 µmol $L^{-1}$ silicate (Si), to provide optimal nutrient conditions (Redfield ratio N:P; 16:1) and prevent Si-limitation. At the onset of the experiment, 0.5 L polycarbonate bottles (Nalgene) filled with 500 mL artificial seawater medium (Kester *et al.* 1967; Guillard 1975) were fixed on a rotating incubator, ensuring the mixing of the bottle content (34 sec per rotation) (Figure 2). To simultaneously investigate both the plastic aspect of intraspecific variability and variability among genotypes, seven different nitrate treatments (hereafter referred to as N treatments) were independently applied to the nine genotypes (Figure 1). While phosphate concentration was kept constant across all treatments with 2.0 µmol $L^{-1}$, nitrate levels were adjusted to 2.5, 5, 7.5, 12.5, 20, 30, and 40 µmol $L^{-1}$ (Table 1), creating regimes that covered strong nitrate-limited conditions up to Redfield ratio in nutrient supply (Redfield *et al.* 1963). Silicate concentrations were adapted to a 1.5:1 Si: N ratio across all treatments. Selenium, trace metals, and vitamins were held constant across treatments according to Kester *et al.* (1967). After the acclimation phase, each bottle was inoculated with approximately 250 cells $mL^{-1}$ in a fully crossed way, such that each of the nine genotypes was treated with the seven different nitrate concentrations with triplicates each, resulting in 189 experimental units (Table 1). Additionally, three bottles containing only medium, but no cells were added on the plankton wheel as 'blanks' to control for nutrient uptake other than by phytoplankton. The light was supplied in a 17:7h light: dark cycle (3-hour sunrise and sunset, respectively) with 299.6 ± 21 µmol $m^{-2}$ $s^{-1}$ at maximum light intensity. The experiment ran for seven days in a climate chamber at a constant temperature of 20°C.

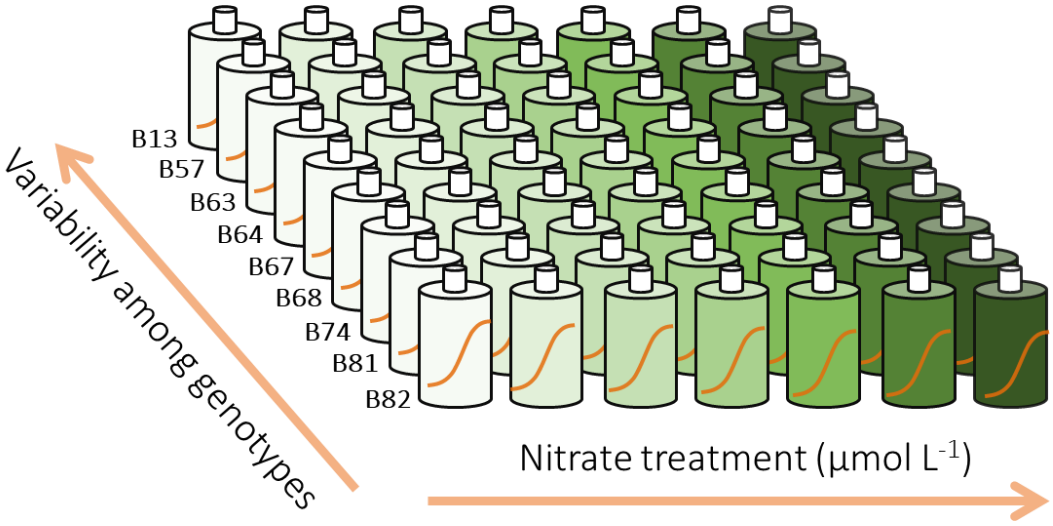


***Figure 1**: Experimental design.*

***Figure 2**: Experimental setup with bottles on the rotating incubator (picture by J.Hamer).*

***Table 1**: Treatment combinations.*

| Genotypes (9) | Nutrient supply of treatments [µmol L$^{-1}$] | | | | | | |
|---|---|---|---|---|---|---|---|
| | 2.5N:2P | 5N:2P | 7.5N:2P | 12.5N:2P | 20N:2P | 30N:2P ~ Redfield ratio | 40N:2P |
| B13, B57, B63, B64, B67, B68, B72, B81, B82 | 9x3 | 9x3 | 9x3 | 9x3 | 9x3 | 9x3 | 9x3 |

## Sampling

The bottles were sampled daily under a biosafety cabinet (AZBIL TELSTAR, model: Bio-II-Advance 4) for measurements of cell abundance and size. For cell abundance and size

measurements, a 6 mL volume was sampled and fixed with Lugol's iodine solution. At the end of the experiment (day seven), additional samples were taken for measurements of cellular nutrients. For this purpose, 50 to 220 mL subsamples were filtered on combusted and acid-washed GF/F filters (Whatman, Germany) using a water jet pump. Two filters per bottle were sampled, one for particulate organic carbon (POC): particulate organic nitrogen (PON)-analysis (C:N) and one for particulate organic phosphorus (POP), respectively.

## Sample preparation and analysis

The cells were counted, and cell size was measured using an inverted microscope (Axiovert 200) after sedimentation (2 h) in Utermöhl chambers. Samples were counted at 200-fold magnification in full chamber transects until at least 400 cells and two transects were counted. The apical d (width) and pervalvar (length) axis h of five randomly chosen cells was measured under 400-fold magnification using an Axiocam 305 and ZEN blue 3.2 software (Zeiss, Version 3.2.0.0000). The arithmetic mean of the measured axes was created to calculate the mean cell size V (biovolume) according to Hillebrand *et al.* (1999):

Equation 1: Cell size (Biovolume; V)

$$V = \frac{\pi}{4} * d^2 * h$$

The filters for the cellular nutrient samples were dried at 60 °C for 24h in a drying cabinet (Memmert, type UNE 400) and stored in desiccators until further analyses. The POC: PON filters were folded into tin foils and transported to the University of Oldenburg for the elemental analysis, which was performed using a CHN analyzer (Thermo, Flash EA 1112). The POP samples were combusted, transferred in 5 mL Pyrex glass tubes (Duran Group, GL 14), dissolved in 4.5 molar sulphuric acid, and further diluted before being measured using a QuAAtro39 autoanalyzer (SEAL) by a technician who provided the analysis output.

## Statistical analysis

All analysed variables and datasets were statistically tested for normal distribution of residuals and homogeneity of variance. If assumptions were not met, data were natural log-transformed. Assumptions of tests were validated graphically, and the significance level for the analyses was set to $p<0.05$. Genotype B68 was excluded from the analysis as

it deviated significantly from the other genotypes in terms of cell size, and after applying Cook's Distance test, was treated as an outlier. To test for intergenotypic variability, a linear model testing for the main effects of genotype identity as a categorical factor, N treatment as a continuous factor set as both linear and quadratic terms, and potential interactions among the two factors were tested on cell size, cellular nutrients, and stoichiometry. Initially, six models were designed, starting from the most complex model (with all possible interactions among the factors, Table 2), from which model selection towards careful model simplification was applied. The model selection followed biological reasoning and the Akaike information criterion (AIC). Subsequently, an Analysis of Covariance (ANCOVA) was performed on the selected model. The final model output was reported using ANOVA type III.

To test for each genotype's plasticity in the response variables, the factor N treatment was tested for each genotype separately by fitting linear or quadratic models, according to AIC model selection, and performing a linear regression per variable and genotype. To test for possible interrelations between cell size and cellular nutrient content and C:N ratios, correlations were performed using Pearson's Product Moment Correlation. To account for multiple hypothesis testing across each genotype and decrease the false discovery rate, the statistical outcomes were corrected using the Benjamini-Hochberg procedure (Benjamini & Hochberg 1995).

All statistical analyses were done using R software (R Development Core Team 2021) and additional packages ggpubr (Kassambara 2022), psych (Revelle 2022), car (Fox & Weisberg 2019), plyr (Wickham 2011), ggplot2 (Wickham 2016), dplyr (Wickham *et al.* 2022), RColorBrewer (Neuwirth & Brewer 2014) and scales (Wickham & Seidel 2022).

***Table 2**: Designed models used for model selection with nitrate treatment ($N_t$) as continuous factor, and genotype identity (G) as categorical factor.*

| **Model** | **Model formula** |
|---|---|
| model_1 | lm(Parameter ~ $N_t$ + $N_t^2$ + G + $N_t$:G + $N_t^2$:G, df) |
| model_2a | lm(Parameter ~ $N_t$ + $N_t^2$ + G + $N_t$:G, df) |
| model_2b | lm(Parameter ~ $N_t$ + $N_t^2$ + G + $N_t^2$:G, df) |
| model_3 | lm(Parameter ~ $N_t$ + $N_t^2$ + G, df) |
| model_4a | lm(Parameter ~ $N_t$ + G + $N_t$:G, df) |
| model_4b | lm(Parameter ~ $N_t$ + G, df) |

# 3|Results

## Cell size

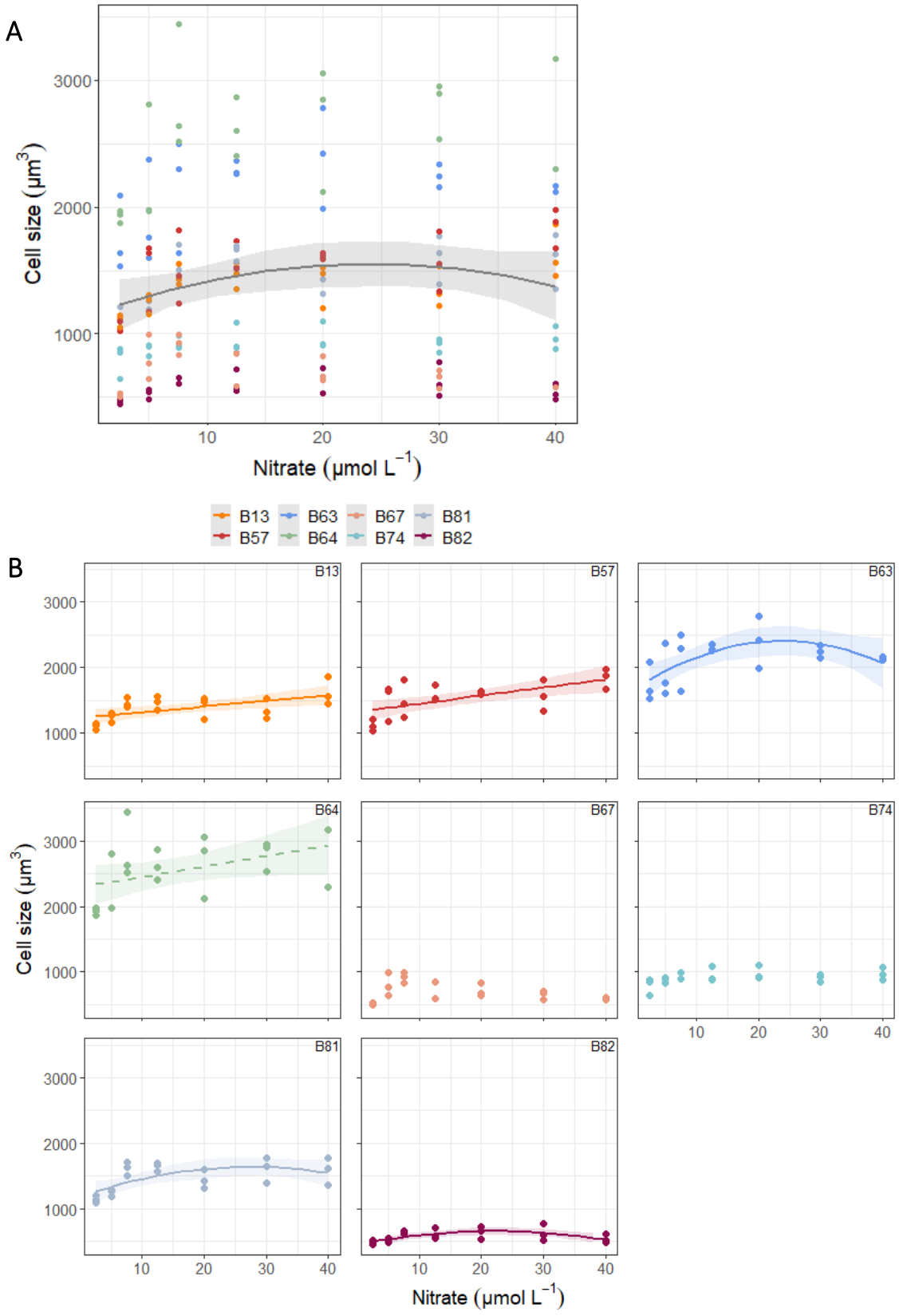


***Figure 3***: *A: Variability among genotypes of cell size. B: Plasticity of cell size in response to the N treatment of each of the eight genotypes. Colors indicate genotype identity. Line type indicates significance level of the fitted model: solid line ($p \leq 0.05$), dashed line ($0.05 \leq p \geq 0.1$), no model fitted indicates non-significant. model output.*

On the intergenotypic level, mean cell size was significantly affected by the genotype identity, N treatment, and the interaction of both (Table 3). Mean cell size in response to increasing N concentration showed a hump-shaped pattern with maximum cell size in 20 and 30 µmol N $L^{-1}$. Across all genotypes, the mean cell size varied between 1100 $\mu m^3$ and 1550 $\mu m^3$ (Figure 3A). The 30 µmol N $L^{-1}$ treatment is considered as close to optimal conditions (Redfield ratio in supplied nutrients of 16N:1P). The interaction term between genotype identity and N treatment indicated that the response to the N treatment depended on the genotype identity and therefore the form of the response curves of the genotypes differed. In particular, three genotypes (B63, B81, B82) showed a significant hump-shaped response in cell size to the N treatment, two (B13, B57) a significant linear increase, one (B64) a trend of increase, and two genotypes (B67, B74) no significant response (Figure 3B).

Besides the different reaction norms, the genotypes differed in their plasticity in cell size. Genotype B82 shows plasticity in size of about 250 $\mu m^3$, whereas other genotypes, like B13, were plastic in a range of about 700 $\mu m^3$ and B57, B63 and B64 were able to span a maximum of 1000 $\mu m^3$ in the plasticity of cell size in response to the N treatment (Figure3B). In addition to this intragenotypic variability, the mean cell size of the genotypes differed significantly from another, varying between 500 $\mu m^3$ to 3000 $\mu m^3$.

*Table 3: ANCOVA type III model output of cell size in response to the N treatment.*

Size ($R^2_{adj}$: 0.894, F= 87.44, p= < 2.2e-16 ***)

Anova Table (Type III tests)

Response: Size_cell_um3

| | Sum Sq | Df | F value | Pr(>F) | |
|---|---|---|---|---|---|
| Nitrate_treatment | 1070768 | 1 | 21.8344 | 6.625e-06 | *** |
| I(Nitrate_treatment^2) | 826437 | 1 | 16.8522 | 6.655e-05 | *** |
| Genotype | 18796251 | 7 | 54.7544 | < 2.2e-16 | *** |
| Nitrate_treatment:Genotype | 878262 | 7 | 2.5584 | 0.01623 | * |

---

Signif. codes: 0 ‘***’ 0.001 ‘**’ 0.01 ‘*’ 0.05 ‘.’ 0.1 ‘ ’ 1

## Particulates per cell

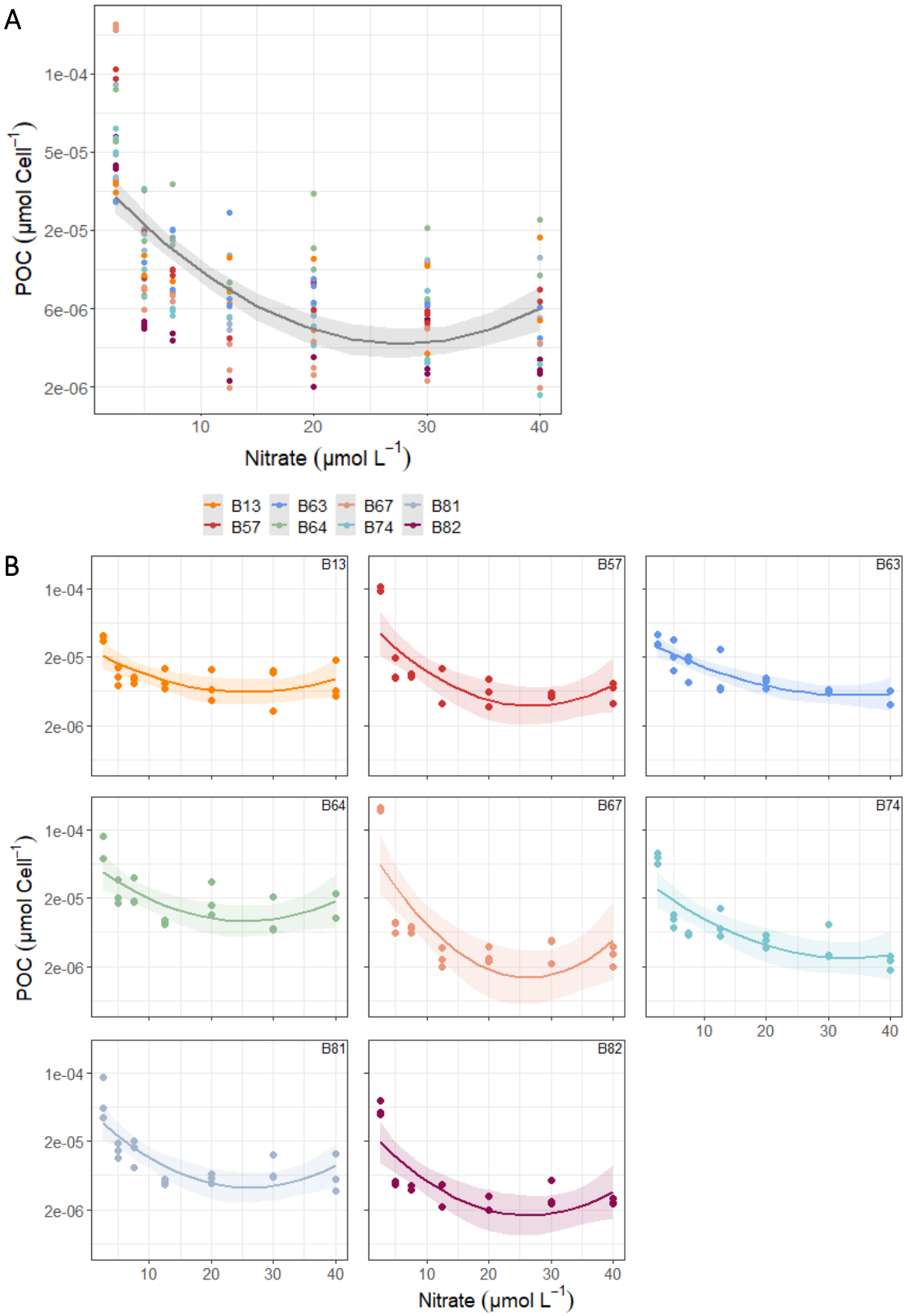


***Figure 4***: *A: Variability among genotypes of particulate organic carbon per cell (POC). B: Plasticity of POC per cell in response to the N treatment of eight genotypes. Colors refer to genotype identity. Line type indicates significance level of the fitted model: solid line ($p \leq 0.05$), dashed line ($0.05 \leq p \geq 0.1$).*

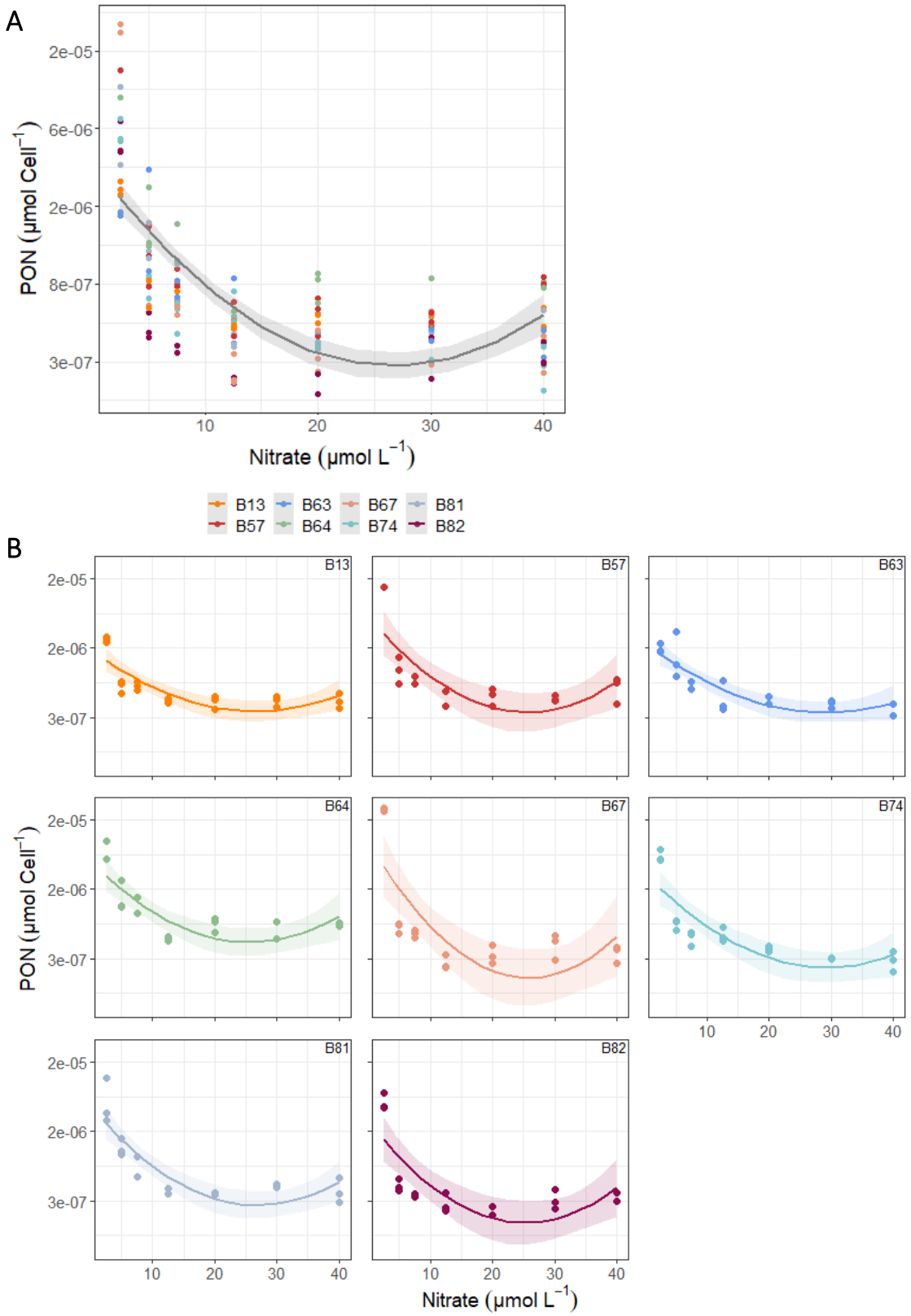


***Figure 5**: A: Variability among genotypes of particulate organic nitrogen per cell (PON). B: Plasticity of PON per cell in response to the N treatment of eight genotypes. Colors refer to genotype identity. Line type indicates significance level of the fitted model: solid line ($p \leq 0.05$), dashed line ($0.05 \leq p \geq 0.1$).*

Across all genotypes, both, mean cellular POC and PON were significantly affected by genotype identity and N treatment (Table 4) and responded in a U-shaped pattern with increasing N concentration (Figures 4 & 5). Therefore, the cellular nutrients were highest in the lowest (2.5 µmol N $L^{-1}$) N treatments and lowest at intermediate (20 and 30 µmol N $L^{-1}$) levels. The genotypes revealed differences in the total amount of cellular nutrients accumulated per cell, as well as across the N treatments reflected by significant effects of the N treatment, and genotype identity in response to the N treatment (Table 4). In contrast to cell size, there was no significant interaction between N treatment and genotype identity in either POC or PON, resulting in uniform response curves for each genotype in response to the N treatment (Figures 4B & 5B).

***Table 4****: ANCOVA type III model output of cellular nutrients (POC and PON) in response to the N treatment.*

POC ($R^2_{adj}$: 0.5357, F = 21.51, p= < 2.2e-16 ***)

```
Anova Table (Type III tests)

Response: ln_Conc_mumol_Cell_POC
                      Sum Sq  Df   F value    Pr(>F)
Nitrate_treatment      41.13   1   94.8910 < 2.2e-16 ***
I(Nitrate_treatment^2) 24.96   1   57.5862 3.096e-12 ***
Genotype               16.27   7    5.3613 1.679e-05 ***
---
Signif. codes:  0 ‘***’ 0.001 ‘**’ 0.01 ‘*’ 0.05 ‘.’ 0.1 ‘ ’ 1
```

PON ($R^2_{adj}$: 0.5969, F = 27.33, p= < 2.2e-16 ***)

```
Anova Table (Type III tests)

Response: ln_Conc_mumol_Cell_PON
                      Sum Sq  Df   F value    Pr(>F)
Nitrate_treatment      58.64   1  149.5967 < 2.2e-16 ***
I(Nitrate_treatment^2) 37.83   1   96.5116 < 2.2e-16 ***
Genotype                9.11   7    3.3199  0.002573 **
---
Signif. codes:  0 ‘***’ 0.001 ‘**’ 0.01 ‘*’ 0.05 ‘.’ 0.1 ‘ ’ 1
```

## Stoichiometry

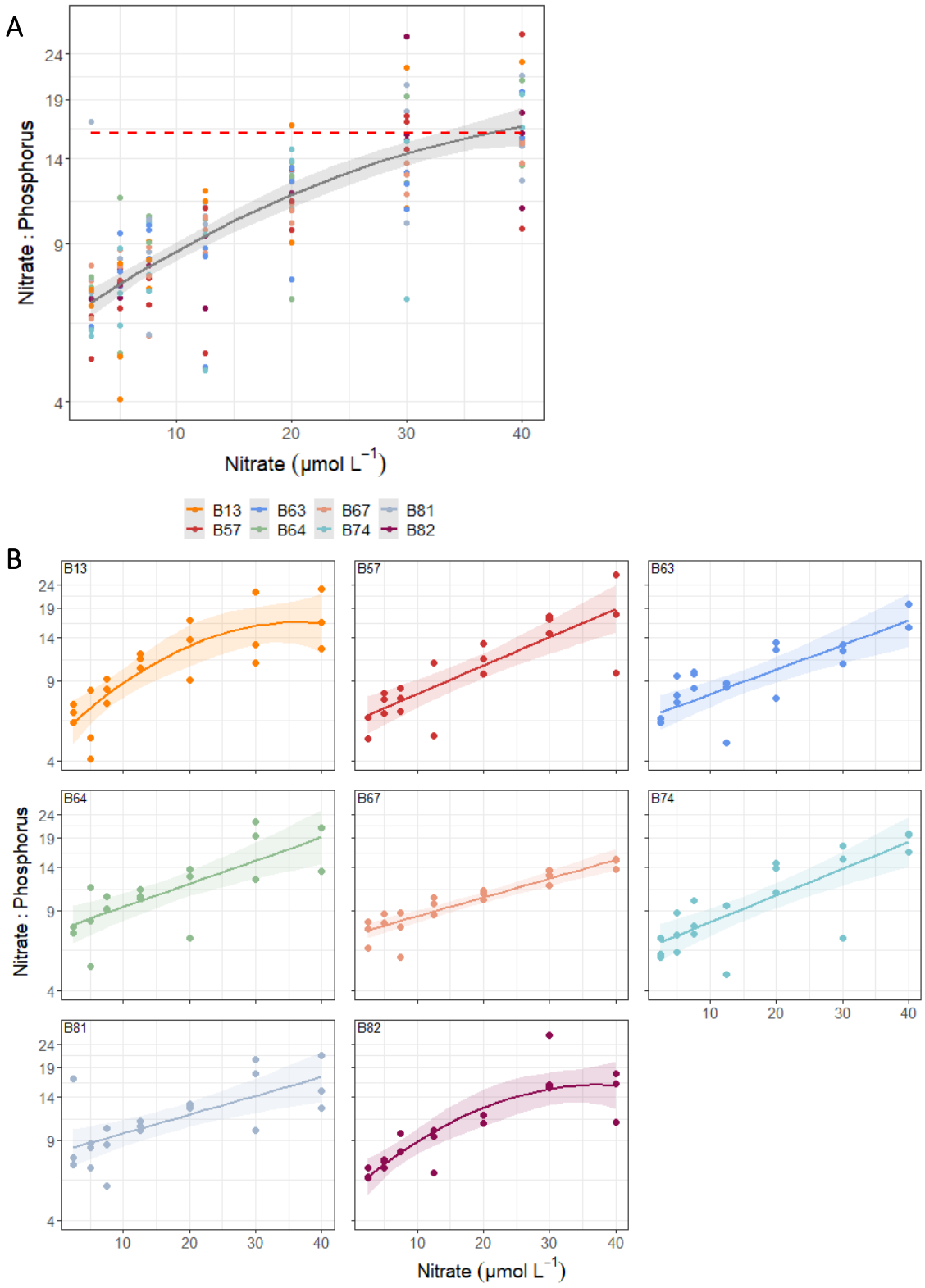


***Figure 6**: A: Variability among genotypes in Nitrate: Phosphorus (N: P) ratio. Red dashed line indicates intracellular Redfield ratio (16:1) B: Plasticity of N: P ratio in response to the N treatment of eight genotypes. Colors refer to genotype identity. Line type indicates significance level of the fitted model: solid line ($p \leq 0.05$), dashed line ($0.05 \leq p \geq 0.1$).*

*Table 5: ANCOVA type III model output of cellular stoichiometry (N:P and C:N) in response to the N treatment.*

NP ($R^2_{adj}$: 0.6367, F= 32.16, p= < 2.2e-16 ***)

```
Anova Table (Type III tests)

Response: ln_Ratio_NP
                     Sum Sq  Df  F value    Pr(>F)
Nitrate_treatment     2.328   1  39.8793 2.865e-09 ***
I(Nitrate_treatment^2)  0.364   1   6.2336   0.01361 *
Genotype              0.526   7   1.2862   0.26076
---
Signif. codes:  0 ‘***’ 0.001 ‘**’ 0.01 ‘*’ 0.05 ‘.’ 0.1 ‘ ’ 1
```

CN ($R^2_{adj}$: 0.4358, F=8.724, p= 1.448e-14***)

```
Anova Table (Type III tests)

Response: ln_Ratio_CN
                       Sum Sq  Df  F value    Pr(>F)
Nitrate_treatment       1.612   1  36.6979 1.145e-08 ***
I(Nitrate_treatment^2)  1.305   1  29.7096 2.123e-07 ***
Genotype                0.406   7   1.3222  0.243873
Nitrate_treatment:Genotype  0.915   7   2.9762  0.006043 **
---
Signif. codes:  0 ‘***’ 0.001 ‘**’ 0.01 ‘*’ 0.05 ‘.’ 0.1 ‘ ’ 1
```

The cellular molar nitrogen-to-phosphorus ratio (N:P) was significantly affected by the N treatment, and as the genotypic effect in the main model was not significant, the genotypes did not differ in the cellular N:P in response to the N treatment (Table 5). The N:P ratio across genotypes in response to the N treatments showed a saturating pattern increasing from values of 3.8 up to 26.6 towards the highest N treatment (Figure 6A). As the red dashed line indicates the intracellular Redfield ratio (16:1 N:P) according to literature (Redfield et al., 1963), all treatment levels except for the highest were considered nitrate-limited.

As no significant interaction was given by the model, all genotypes responded in a very similar and unidirectional pattern. Precisely, two genotypes (B13, B82) showed a significant saturating response curve, while the other six showed a significant linear response to increasing N concentrations (Figure 6B).

To further quantify the limitation indicated by N:P, I looked at the C:N ratio in response to the N treatment. The C:N ratio was significantly affected by the N treatment and the interaction of genotype identity and N treatment, whereas the genotype identity alone had no significant effect on C:N in response to the N treatment (Table 5). Over all genotypes, a hump-shaped reaction norm of C:N was observed across the N treatments

(Figure 7A). Interestingly, the cells became more nitrate-limited with increasing N supply at intermediate treatments (20 µmol N $L^{-1}$), and C:N decreased towards optimal conditions (30 to 40 µmol N $L^{-1}$; highest N treatment). Therefore, the C:N ratio was low at minimal N supply as well as in the highest N treatments.

The statistically observed intragenotypic variability in the main model, indicated by the significant interaction term, translated to different forms of reaction norms when the response variable was considered separately by genotype identity. Four genotypes showed a significant (solid line; B81) or marginally significant (dashed line; B63, B64, B74) hump-shaped nitrate limitation that decreased with increasing N supply. In contrast, the cellular C:N of B81 increased across the N treatments and two genotypes (B13, B57) had no significant response in C:N with increasing N supply.

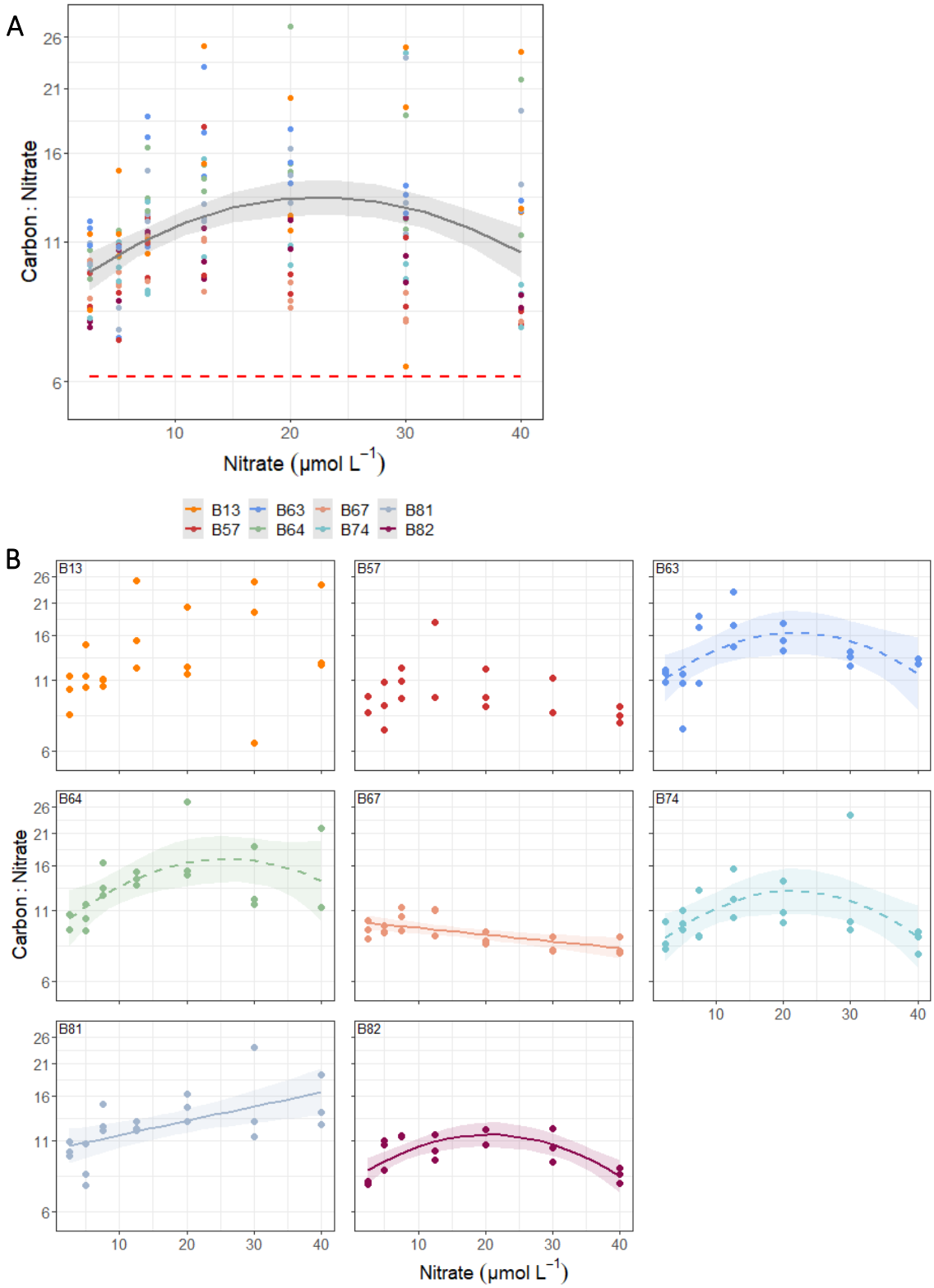


*Figure 7: A: Variability among genotypes in Carbon: Nitrate (C: N) ratio. Red dashed line indicates intracellular Redfield ratio (6.6 (106:16)) B: Plasticity of C: N ratio in response to the N treatment of eight genotypes. Colors refer to genotype identity. Line type indicates significance level of the fitted model: solid line ($p \leq 0.05$), dashed line ($0.05 \leq p \geq 0.1$), no model fitted indicates non-significant. model output.*

## Correlations

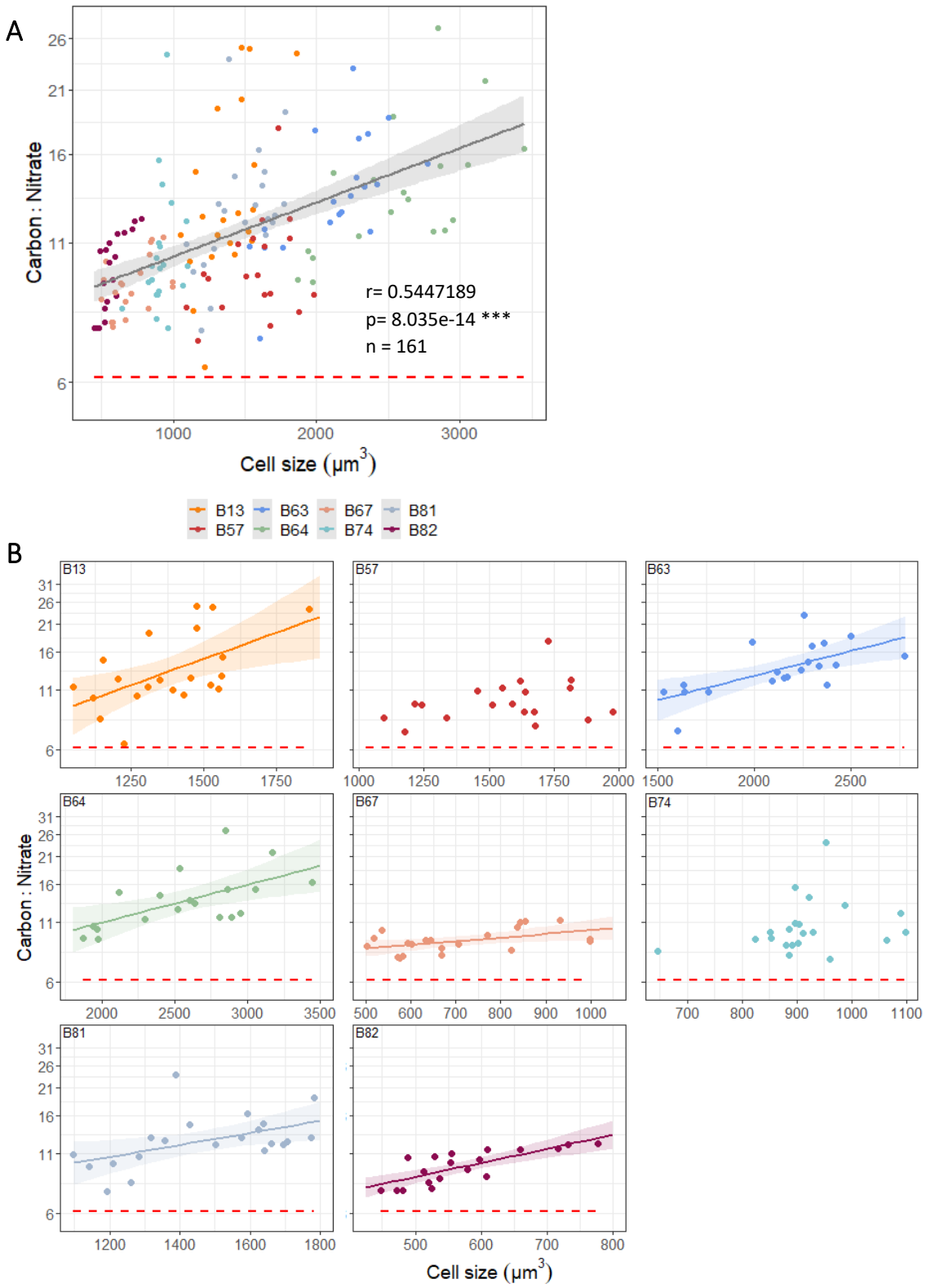


***Figure 8***: *Correlation among genotypes of cell size with (A) pooled Carbon: Nitrate ratio, and (B) split by genotype identity. Red dashed line indicated intracellular Redfield ratio (6.6 (106:16)). Colors represent genotype identity. Line type indicates significance level of correlation coefficient: solid line ($p \leq 0.05$), dashed line ($0.05 \leq p \geq 0.1$), no model fitted indicates non-significant. model output. Correlation coefficients see Table 6.*

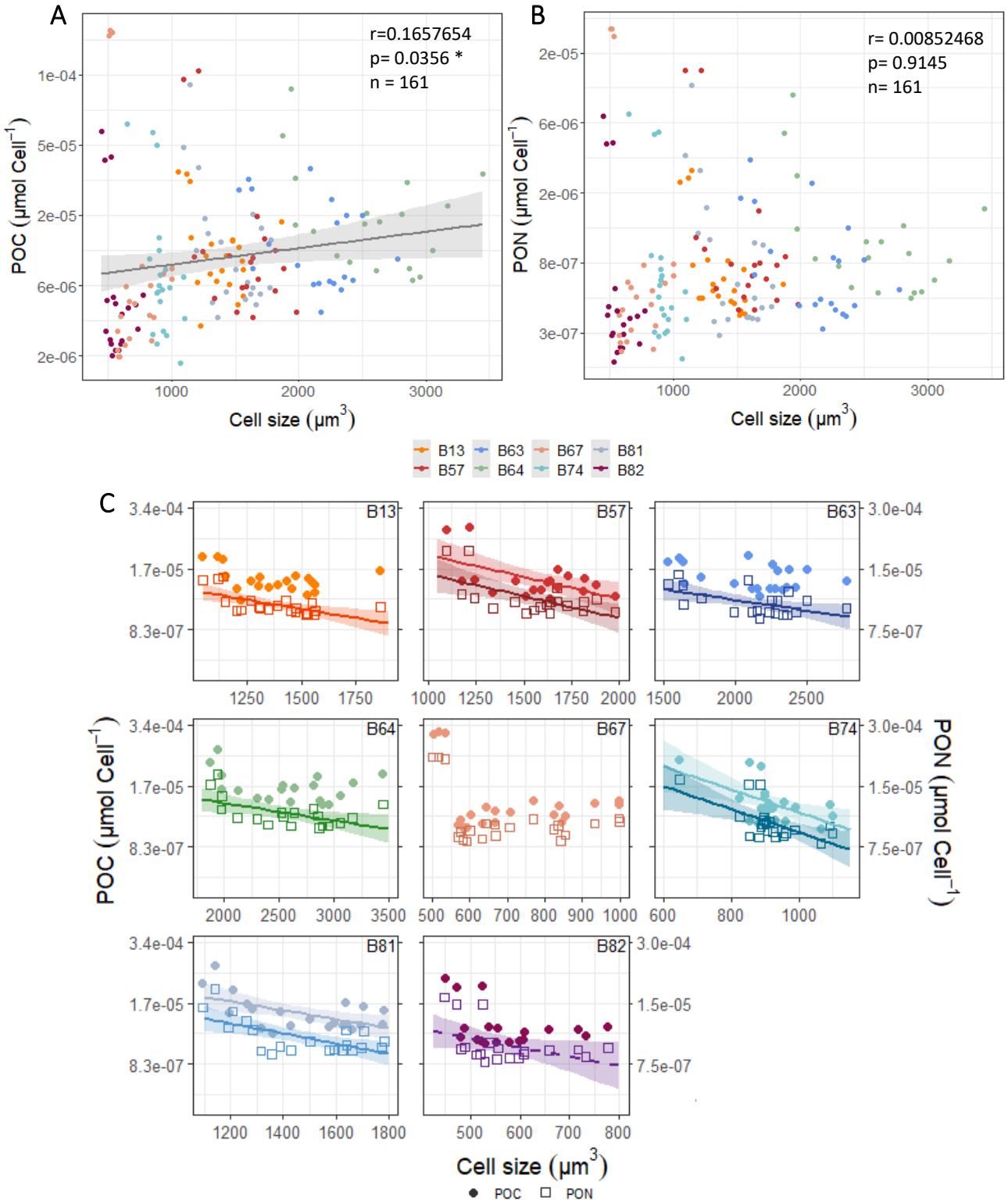


*Figure 9*: *Correlation among genotypes of cell size with (A) POC, (B) PON and (C) split by genotype identity. Correlation of cell size and POC (primary y axis, indicated by filled dots) and PON (secondary y axis, indicated by open squares and darker color shade). Colors represent genotype identity. Line type indicates significance level of correlation coefficient: solid line ($p \leq 0.05$), dashed line ($0.05 \leq p \geq 0.1$), no model fitted indicates non-significant. model output. Correlation coefficients see Table 7.*

As we observed the same pattern in C:N and cell size in response to the N treatment, we hypothesized that the cellular nutrients may be related to or mediated by cell size. To test this hypothesis correlations of cell size with the stoichiometry and the cellular nutrients were performed.

The correlation of cell size to C:N revealed that within and across different genotypes the nitrate limitation increased with increasing cell size (Figure 8). Overall, the genotypes showed a significant correlation between C:N and cell size ($r = 0.545$, $p \leq 0.0001$ ***, Figure 8A), which corresponded to the differences in accumulated cellular nutrient content. This translated to lower C:N ratios in smaller cells due to higher PON content per cell, and higher C:N ratios in larger cells. The C:N ratios in six out of eight genotypes significantly correlated positively with cell size (Table 6). Consequently, at inter- and intragenotypic level small cells were the least N-limited.

To disentangle the responsible element for the intraspecific correlations between cell size and C:N ratio, I looked separately at the correlations of cell size with POC and PON, respectively. Across all genotypes, cell size and POC per cell were significantly positively correlated with a correlation coefficient of $r = 0.166$ ($p \leq 0.05$ *) (Figure 9A), while size and PON were not correlated (Figure 9B). Hence, I concluded that across all genotypes the correlation between cell size and C:N was likely C driven. Interestingly, for both elements, many small cells which accumulated less nutrients and few that contained higher amounts were observed (Figure 9 (A, B, C)). This 'bifurcation' in the data occurred across all genotypes, resulting in weak or no statistically significant correlation of POC and PON per cell with cell size (high cellular nutrients in low N-supply treatments).

Even though there was weak or no correlation on the intergenotypic level, on the plasticity level the genotypes showed a unidirectional response of cell size to cellular nutrients. The pattern, however, switched from the intergenotypically positive correlation to an intragenotypically negative correlation of cell size with POC and PON, respectively (Figure 9C). Hence POC (filled dots) and PON (open squares) declined with increasing cell size (Figure 9C). Therefore, the smallest cells within each genotype had the highest cellular nutrient contents.

Precisely, cellular nitrogen was significantly negatively correlated with cell size in seven out of eight genotypes, whereas cellular carbon significantly declined with increasing cell

size in three out of eight genotypes (B57, B74, and B81). In general, PON per cell experienced a more pronounced change with increasing cell size compared to POC, which is reflected in a steeper slope in the correlation with cell size (Table 7). In the case of the three genotypes, in which both cellular nutrients were significantly correlated with size, r for PON was smaller than for POC. Thus, the data suggested, that the PON content per cell declined stronger with increasing cell size.

*Table 6: Pearson's product-moment correlation output and significance level of cell size and cellular stoichiometry (C:N).*

| Genotype | C:N [-] |
|---|---|
| B13 | r = 0.5588244, p = 0.01691 * |
| B57 | r = 0.3150403, p = 0.215885714 n.s. |
| B63 | r = 0.6482345, p = 0.007976 ** |
| B64 | r = 0.6080902, p = 0.015309333 * |
| B67 | r = 0.4971616, p = 0.029133333 * |
| B74 | r = 0.2469335, p = 0.2805 n.s. |
| B81 | r = 0.5056954, p = 0.03096 * |
| B82 | r = 0.7736762, p = 0.0008152 *** |

*Table 7: Pearson's product-moment correlation output and significance level of cell size and cellular nutrients (POC and PON).*

| Genotype | POC [µmol cell$^{-1}$] | PON [µmol cell$^{-1}$] |
|---|---|---|
| B13 | r =-0.3355240, p = 0.182666667 | r =-0.5187680, p = 0.009976 ** |
| B57 | r =-0.5588102, p = 0.034346667 * | r =-0.6087593, p = 0.011346 * |
| B63 | r =-0.3784331, p = 0.19982 | r =-0.5517319, p = 0.018672 * |
| B64 | r =-0.3700796, p = 0.19024 | r =-0.5436258, p = 0.02152 * |
| B67 | r =-0.3222771, p = 0.1542 | r =-0.3633731, p = 0.1054 |
| B74 | r =-0.5769596, p = 0.049408 * | r =-0.6172935, p = 0.007656 ** |
| B81 | r =-0.5699643, p = 0.027944 * | r =-0.6391034, p = 0.01452 * |
| B82 | r =-0.3433091, p = 0.171542857 | r =-0.4300068, p = 0.075565714 . |

# 4|Discussion

The data of my thesis clearly show that both differences among genotypes and phenotypic plasticity contributed to the intraspecific variability in cell size, cellular nutrient content, and stoichiometry. Referring to hypotheses 1 and 2, I found a unimodal hump-shaped pattern for the response variables cell size and C:N ratio across all genotypes in response to the N treatments. This pattern, however, did not hold for the single genotypes, meaning the plasticity level. In contrast, I observed a U-shaped pattern for the cellular nutrient content of POC and PON across all genotypes in response to increasing N supply. This pattern was the same for both levels of intraspecific variability, phenotypic plasticity, and the variability among genotypes. Referring to hypothesis 3, I found that cell size correlated negatively with POC and PON at the plasticity level, but partly positively at the intergenotypic level. On both levels, however, cell size correlated positively with C:N, suggesting that cell size may mediate the response of cellular nutrient content and C:N ratio to N supply.

## Effects of manipulated nitrate concentration on trait variation

The observed unimodal response of cell size with increasing N concentration is an interesting aspect of this study. Based on the fact that nutrient limitation has been found to lead to smaller cells or a decrease in organism size (Marañón *et al.* 2013; Sommer *et al.* 2016; Hillebrand *et al.* 2022), I generally expected a linear positive relationship between N concentration and cell size. Surprisingly, I found that across all genotypes cell size showed a hump-shaped response to increasing nutrients, which means that the expected cell size increase with N concentration was followed by a decline (Figure 3A). Considering the plastic responses of single genotypes only, however, I found various shapes of reaction norms along the gradient of N supply (Figure 3B). While some of the genotypes responded as expected to the increasing N supply, others showed a hump-shaped pattern. A possible explanation for the hump-shaped responses could be that some genotypes already experienced P-limitation in the highest N treatments, while the genotypes with a linear increase in cell size were not yet limited. These differences in the plastic response pattern of cell size to N supply translated to the overall hump-shaped response among all genotypes (referring to hypotheses 1 and 2). The effects of potential

P-limitation in the highest N treatment on cellular C:N will be discussed in the following paragraphs.

In line with hypotheses 1 and 2, the cellular concentrations of POC and PON were affected by the N treatment on both levels, phenotypic plasticity, and among the genotypes. The first half of the consistent U-shaped response of cellular POC and PON content to N supply is not surprising, because the cells utilised the available nutrients from the medium through vegetative reproduction to build up new biomass (Figures 4&5 A&B). As the increasing N supply allowed for more cell divisions and hence higher biomass, the cellular nutrient content likely decreased, because the available nutrients were shared between more cells. Based on this explanation the slight cellular nutrient increase with further increasing supply was unexpected. I can only speculate about the reason. One possibility is that the overall smaller cell size in the highest N treatment in response to the manipulated N supply allowed for slightly higher cellular nutrient content in relation to the total cell volume. I will further discuss this aspect below. Another influencing factor in combination with cell size that can additionally explain the cellular PON but not the POC increase at the highest N supply is that cell abundance flattened at the highest N supply thus it did not significantly differ from the 30N treatment (Figure A 1). This means the same number of smaller cells might have accumulated the higher content of nitrate.

Stoichiometric data can be an indicator of potential nutrient stress. The Redfield ratio of N:P of 16:1 became a benchmark in stoichiometry. Deviations indicate which of the two nutrients is likely limiting (type of limitation) (Choudhury & Bhadury 2015; Falkowski 1997; Tyrrell 1999; Lenton & Watson 2000). Therefore, it is assumed that phytoplankton is N-limited at N:P < 16, and that it is P-limited at N:P > 16 (Geider & La Roche 2002). My data show that the N:P ratio increased unimodally in response to the N treatment from a ratio of ~ 6.5 towards the Redfield ratio, which it slightly exceeded at the highest N supply (~ 18) (Figure 6A). This pattern held for both intraspecific variability aspects (supporting hypotheses 1 and 2), which means that I can confirm that almost all replicates can be considered nitrate-limited, with values significantly lower than the Redfield ratio (Redfield *et al.* 1963). Despite the fact that the treatments 30 µmol N $L^{-1}$ and 40 µmol N $L^{-1}$ were close to Redfield conditions, I do not know yet if this particular ratio (16:1) applies to my genotypes of *Chaetoceros affinis* or even the species in terms of decisive ratio for the identification of (co-)limitation. After identification of the type of limitation, which in

my case is N-limitation, Goldman *et al.* (1979) and Peter & Sommer (2013) proposed that the C:N ratio can serve as a proxy for the strength of N-limitation. This is because the cellular C:N ratio is the inverse of the carbon-normalized N-cell quota (Droop 1973) and shows a linear relationship to the extent of nutrient limitation (Goldman *et al.* 1979). Based on these considerations, my data on cellular stoichiometry suggest nitrate limitation, which surprisingly increased with increasing N supply, peaked at intermediate supply and decreased towards higher N treatments. Moreover, I observed this counterintuitive pattern in both, partly in phenotypic plasticity, and variability among genotypes (referring to hypotheses 1 and 2).

The hump-shaped response across the genotypes and the intragenotypically different reaction norms of the plastic responses for C:N in response to increasing N supply (Figure 7A&B) differed from the expectation deduced from the literature. According to previous research, the C:N ratio decreases with increasing N supply because cells can downregulate the synthesis of N-rich protein content under nutrient limitation, while at high N-concentrations phytoplankton can store excess nitrate intracellularly as protein or free amino acids (Grosse *et al.* 2017; Liefer *et al.* 2019; Sterner & Elser 2002; Tanioka & Matsumoto 2020).

One reason for the unexpected pattern may be that the C:N ratio is known to vary with a variety of environmental factors and is species-specific (Marañón 2015; Inomura *et al.* 2020; Finkel *et al.* 2010). Therefore, it cannot be generalized to an exact ratio that determines the strength of a limitation. Theoretically, however, there are possibilities to calculate the strength of limitation indicated by the C:N ratio to allow comparability between, for example, different genotypes or species under the same experimental conditions or even different environmental gradients. One approach requires the growth rate $\mu_{actual}$ of a specific genotype from the day the cellular nutrients were measured and its maximum growth rate $\mu_{max(treatment)}$ under the treatment conditions of the experiment. The quotient of the two rates then determines the strength of the limitation (Bucciarelli *et al.* 2010). If $\frac{\mu_{actual}}{\mu_{max(treatment)}} = 1$ there is no limitation. The stronger the limitation is, the closer the value is to 0. Unfortunately, this calculation was not possible for this study, because the necessary data for this analysis have not been measured.

## Potential consequences of cell size for observed trait variation

Another possible explanation for the unexpected hump-shaped response in C:N in response to the N treatment might be the differences in cell size which showed a similar pattern in response to the experimental N gradient and thus could have mediated the pattern in C:N (referring to hypothesis 3). Precisely, the positive correlation of cell size and C:N is in line with my third hypothesis and suggests that cell size potentially mediates stoichiometry and the observed variability, within and across different genotypes, thus also supporting hypothesis 2 (Figure 8A&B). The scaling of stoichiometry with cell size is congruent with interspecific findings of Aksnes & Egge (1991) and Litchman *et al.* (2007), demonstrating that larger cells contain lower cellular nutrient contents, which translates to increasing C:N with increasing cell size. As such my findings are largely consistent with previous studies. Marañón *et al.* (2013), for example, demonstrated a strong positive correlation between cell size and the C:N ratio across different taxonomic groups. In comparison, my data confirm that this pattern also holds intraspecifically between and within the genotypes of a single species.

Marañón *et al.* (2013) attribute the lower C:N ratio of smaller cells to minimum requirements for cell growth. More precisely, these are associated with the increasing relative abundance of nitrogen-containing molecules that are part of non-scalable components, such as nucleic acids and membrane proteins (Raven 1994), as well as reduced storage of C-rich compounds such as lipids and carbohydrates (Marañón *et al.* 2013). Consequently, smaller cells are more N-rich, because the non-scalable components occupy a larger fraction of the total cell volume, which minimizes the fraction of cytoplasm available for other C-rich scalable components directly involved in metabolic activity and biomass production (Raven 1994; Marañón *et al.* 2013). These conclusions in turn can explain, why the larger cells in my experiment show higher C:N ratios. The increasing storage capacity in e.g., vacuoles are scaling with cell size (Grover 1991; Stolte & Riegman 1995; Litchman *et al.* 2009), which increases C-rich carbohydrates under N-limited conditions (Liefer *et al.* 2019), resulting in higher C:N ratios. My data suggest that the largest cells experienced the strongest nutrient stress. This observation is based on the occurrence of the largest cells under the strongest N-limitation (C:N data), which in this study was not at the lowest but at intermediate N concentrations and according to N:P are still considered N-limited treatments. Consequently, I assume that

the largest cells exhibited the highest storage capacity and therefore shifted the C:N by accumulating C (Liefer *et al.* 2019).

To investigate the potential role of cell size in explaining the observed pattern in cellular nutrients and C:N in response to the N treatment, I examined the correlation of the parameters with cell size more closely. There is a positive trend in the correlation between cell size and the cellular nutrients (POC and PON) across all genotypes, while the correlation for single genotypes at the level of plasticity was generally negative. Interestingly, I observed a 'bifurcation' in the correlations between cell size and both cellular nutrients among the genotypes. Precisely, I observed two clusters of smaller cells with different cellular nutrient contents, merging into one with increasing cellular nutrient content with increasing cell size (Figure 9A&B). This pattern can be explained by one small cluster containing the cells that were rich in cellular nutrients (POC and PON, upper left in the graph Figure 9A&B), but small in cell size due to nutrient concentration limitation (2.5 N treatment). A second, but larger cluster, consisted of cells of the other N treatments in which the cellular nutrient contents showed a U-shape with N supply but were generally lower than in the 2.5 N treatment. These in the case of POC showed a positive correlation with increasing cell size (Figure 9A). It should be noted that the slight increase in the U-shaped pattern of both cellular nutrients in response to the experimental N gradient in the highest treatment did not form a particular cluster visible in the correlation between size and cellular nutrients. This is because the increase in cellular nutrients at high N supply was not sufficiently different from the cellular nutrients of the larger cells at intermediate N treatments. Furthermore, the cellular nutrient content in the high (40 µmol N L-1) treatment was significantly lower than in the lowest (2.5 N) treatment, which may explain why the replicates of this treatment blended with the larger cluster. The high cellular nutrient content but concentration-limited cluster of small cells in the 2.5 N treatment may have weakened the positive correlation between cell size and cellular nutrients across genotypes, but likely reinforced the consistency of the negative correlations between cell size and cellular nutrient content (Figure 9C). The conclusion, that larger cells accumulate C under stoichiometrically N-limited conditions is also reflected in and supported by the correlations of cell size with the cellular nutrient contents (Figure 9A&B).

Although the correlation was not strong, POC increased intergenotypically with cell size

(Figure 9A), whereas PON did not (Figure 9B), which refers to hypotheses 2 and 3. Moreover, the positive correlation is in line with the results of Hillebrand *et al.* (2022) and suggests that the variability that arose from the differences among the genotypes was driven by C. In contrast, on the plasticity level, the variability seemed to be driven by N, indicated by steeper slopes of PON compared to POC, in case the correlation was significant for both cellular nutrients in each genotype. The findings that the correlation of cell size and cellular nutrient content on the intergenotypic level appeared C driven, whereas intragenotypically was N driven, suggest that the possible relationship between cell size and intracellular C:N ratio was determined by different elements. Previous studies showed that cells can reduce the synthesis of N-rich protein content (mainly proteins and pigments) under N-limitation, resulting in a higher C:N ratio (Liefer *et al.* 2019; Grosse *et al.* 2017; Tanioka & Matsumoto 2020), which may explain why the larger cells, that exhibited stronger limitation, on the plasticity level contained less N in relation to C (Figure 8B & 9C).

## Potentially confounding factors

Even though my results are supported by literature to a certain extent, as discussed above I also found patterns deviating from previous research. My data could potentially be confounded by two different factors: differences in the successional stage of the nutrient-treated genotypes or potential P-limitation in the highest N treatment. In the subsections below, I will discuss the potential confounding factors that could have influenced the observed pattern of my experiment and how one could control for them.

## Successional stage approach

The first potentially confounding factor is that the different genotypes and treatments may not have been in the same successional stage on the last day of the experiment when sampling took place. This is because naturally the treatments with lower N supply enter the stationary phase earlier than the higher N treatments. To evaluate this, the growth curves over the course of the experiment can indicate which genotype reached the stationary phase in its respective treatment. Regarding my data, most of the genotypes reached the stationary phase by the end of the experiment; i.e., depending on the N supply, between days 3 and 4 of the experiment (Figure A 2). This indicates that the successional stage can potentially have affected cellular nutrient content and size.

To control the effects of treatments in terms of potentially confounding effects of different successional stages on my analyses, one could first consider the means of the growth curves (see Appendix, Figure A 2) to determine the onset of the stationary phase for each genotype at each nutrient level. Then, secondly, one can compare the cell sizes and stoichiometric data of these days accordingly. To do so, one would have to measure the cell size, cellular nutrients, and stoichiometry over the course of the experiment. Thereby one could investigate whether the observed pattern in this study is present throughout the experiment or develops over time and would be able to truly compare the data of the same or comparable successional stages. By that, the successional stage cannot confound the data. Due to a lack of data, this issue cannot be resolved in this study but leaves room for future research to do so and further improve the interpretability of the results. If, however, the hump-shaped pattern of cell size in response to the N treatment persists after accounting for potential successional stage differences, I can be confident, that the conclusions drawn from the correlation of cell size and the cellular nutrient content, and of cell size and the stoichiometry also hold.

## Potential P-limitation

The second factor that may have confounded my analyses is the potential P-limitation in the highest N treatment. On the very left side of the gradient is a strong nutrient concentration limitation, and according to the N:P ratio of the supplied nutrients, the treatments are approaching the Redfield ratio and even a bit further. This leads to the question, of whether on the right side of the gradient the ratio of 40N:2P (µmol $L^{-1}$) for my species already means that the cells are P-limited in terms of stoichiometry. One of the genotypes (B64) as a sign of P-limitation of the 40 µmol N $L^{-1}$ treatment, produced higher cell abundances in the 30 µmol N $L^{-1}$ compared to the 40 µmol N $L^{-1}$ treatment in the growth curves (Figure A 2). Since all treatment levels except the 40 µmol N $L^{-1}$ treatment provided nutrients at the Redfield or lower N:P ratio, it was assumed that the 40 µmol N L-1 treatment, may be affected by P-limitation. To test if such potential P-limitation has confounded my conclusions, I excluded the highest N treatment as a conservative assumption and repeated the statistical analyses (Appendix Figures A 3-9 and Tables A 1-5). Generally, neither among the genotypes nor on the plasticity level did the observed pattern change to the extent that it would have affected the conclusions when the potentially confounding treatments were excluded from the analysis. There are

minor changes in statistical outcome in the analysed parameters that will not be discussed in detail. Still in essence the overall pattern in the model among the genotypes stays consistent. On the plasticity level, even though some reaction norms slightly changed their shape, the number of significant responses of cell size and C:N in response to the experimental N gradient even increased, which further strengthens the conclusions derived from the original data. Therefore, the data do not point to a P-limitation to the extent that it largely confounded the conclusions. As such I am confident that the findings of the hump-shaped responses of cell size and C:N with increasing N supply hold. Apart from the exclusion of potentially confounded data, another way to control for potential P-limitation is to take the dissolved nutrient concentrations of the medium over the course of the experiment into account.

## Trustworthiness of consistency

Besides potentially confounding effects on my data, three treatments provide a further indication to trust the observed pattern. The treatments 5 µmol N $L^{-1}$, 7.5 µmol N $L^{-1}$, and 12.5 µmol N $L^{-1}$ can be considered truly comparable, as they are not critical neither in terms of strength of limitation, successional stage nor potential P-limitation. Even though these treatments only represent a subset of the data, the directions and patterns are consistent with the complete data set. That is cell size increases, while cellular nutrients decrease with increasing N supply, and the nutrient limitation (C:N) also increases.

## Implications for future research

My data underpin the general importance to consider intraspecific variability in the nutrient-uptake dynamics of a species previously highlighted by other studies like Malerba *et al.* (2016). Additionally, I propose to take into account the different levels from which the sources of intraspecific trait variability can arise. My results show that intraspecific variability can be significant and that even though not in all, in some cases, such as decreasing cell sizes under nutrient stress, show the same direction as trait variation interspecifically (Aksnes & Egge 1991; Litchman *et al.* 2007; Litchman *et al.* 2015). Moreover, the fact that my data suggest different elemental drivers in variability among genotypes and phenotypic plasticity in the correlation of cell size and stoichiometry, points out that intraspecific variability is not unidimensional. In general, this can mean that intraspecific variability should not be conflated. Instead, the source of

both aspects from which trait variability arises should be considered to account for potentially differing and specific contexts.

# 5|Conclusion

In summary, this study shows that the diatom *Chaetoceros affinis* exhibits variability among genotypes and phenotypic plasticity in cell size, cellular nutrients, and stoichiometry in response to a nutrient gradient. The fact that both cell size and C:N ratio showed hump-shaped responses among genotypes and significantly different reaction norms on the plasticity level in response to increasing nutrients, suggests that cell size plays a role in explaining differences in stoichiometry (C:N). The positive correlation of the two variables underlines the assumption that cell size influences stoichiometry. Furthermore, the positive intergenotypic correlation and negative correlation of cell size with cellular nutrients at the plasticity level suggest that the differences in stoichiometry in response to manipulated nutrients are driven by different elements at the different levels. My data further underpin the importance of considering the different levels from which the sources of intraspecific trait variability can arise. Therefore, it is relevant to ultimately understand the drivers and consequences of intraspecific variation in functionally important groups, such as diatoms. To predict the food web structure in changing environmental conditions in more detail, it may be beneficial to consider intraspecific variability in traits such as cell size and nutrient uptake-related traits. This may ultimately help to assess the capability of phytoplankton groups to cope with climate change and to model the consequences of changes for higher trophic levels or the biological carbon pump.

# 6|References


Aksnes, D.L. & Egge, J.K. (1991). A theoretical model for nutrient uptake in phytoplankton. *Mar. Ecol. Prog. Ser.*, 70, 65–72.

Armbrust, E.V. (2009). The life of diatoms in the world's oceans. *Nature*, 459, 185–192.

Azam, F., Fenchel, T.M., Field, J.G., Gray, J.S., Meyer-Reil, L.-A. & Thingstad, F. (1983). The Ecological Role of Water-Column Microbes in the Sea*. *Marine Ecology Progress Series*, 257–263.

Benjamini, Y. & Hochberg, Y. (1995). Controlling the False Discovery Rate: A Practical and Powerful Approach to Multiple Testing. *Journal of the Royal Statistical Society: Series B (Methodological)*, 57, 289–300.

Benoiston, A.-S., Ibarbalz, F.M., Bittner, L., Guidi, L., Jahn, O. & Dutkiewicz, S. *et al.* (2017). The evolution of diatoms and their biogeochemical functions. *Philosophical transactions of the Royal Society of London. Series B, Biological sciences*, 372.

Bolnick, D.I., Amarasekare, P., Araújo, M.S., Bürger, R., Levine, J.M. & Novak, M. *et al.* (2011). Why intraspecific trait variation matters in community ecology. *Trends in Ecology & Evolution*, 26, 183–192.

Bopp, L., Aumont, O., Cadule, P., Alvain, S. & Gehlen, M. (2005). Response of diatoms distribution to global warming and potential implications: A global model study. *Geophys. Res. Lett.*, 32, n/a-n/a.

Boyd, P.W., Rynearson, T.A., Armstrong, E.A., Fu, F., Hayashi, K. & Hu, Z. *et al.* (2013). Marine phytoplankton temperature versus growth responses from polar to tropical waters--outcome of a scientific community-wide study. *PloS one*, 8, e63091.

Bradshaw, A.D. (1965). Evolutionary Significance of Phenotypic Plasticity in Plants. In: *Advances in genetics* (ed. Caspari, E.W. & Thoday, J.M.). Academic Press, New York, London, pp. 115–155.

Brandenburg, K.M., Krock, B., Klip, H.C.L., Sluijs, A., Garbeva, P. & van de Waal, D.B. (2021). Intraspecific variation in multiple trait responses of Alexandrium ostenfeldii towards elevated pCO2. *Harmful algae*, 101, 101970.

Brown, J.H., Marquet, P.A. & Taper, M.L. (1993). Evolution of body size: consequences of an energetic definition of fitness. *The American Naturalist*, 142, 573–584.

Bucciarelli, E., Pondaven, P. & Sarthou, G. (2010). Effects of an iron-light co-limitation on the elemental composition (Si, C, N) of the marine diatoms *Thalassiosira oceanica* and *Ditylum brightwellii*. *Biogeosciences*, 7, 657–669.

Cervato, C. & Burckle, L. (2003). Pattern of first and last appearance in diatoms: Oceanic circulation and the position of polar fronts during the Cenozoic. *Paleoceanography*, 18, n/a-n/a.

Chisholm, S.W. (1992). Phytoplankton Size. In: *Primary Productivity and Biogeochemical Cycles in the Sea* (ed. Falkowski, P.G., Woodhead, A.D. & Vivirito, K.). Springer US, Boston, MA, s.l., pp. 213–237.

Choudhury, A.K. & Bhadury, P. (2015). *Relationship between N : P : Si ratio and phytoplankton community composition in a tropical estuarine mangrove ecosystem*.

Des Roches, S., Post, D.M., Turley, N.E., Bailey, J.K., Hendry, A.P. & Kinnison, M.T. *et al.* (2018). The ecological importance of intraspecific variation. *Nature ecology & evolution*, 2, 57–64.

Droop, M.R. (1973). Some thoughts on nutrient limitation in algae. *Journal of phycology*, 9, 264–272.

Edwards, K.F., Thomas, M.K., Klausmeier, C.A. & Litchman, E. (2012). Allometric scaling and taxonomic variation in nutrient utilization traits and maximum growth rate of phytoplankton. *Limnol Oceanogr*, 57, 554–566.

Ellison, A.M. (2001). Interspecific and intraspecific variation in seed size and germination requirements of Sarracenia (Sarraceniaceae). *Am. J. Bot.*, 88, 429–437.

Fajardo, A. & Piper, F.I. (2011). Intraspecific trait variation and covariation in a widespread tree species (Nothofagus pumilio) in southern Chile. *The New phytologist*, 189, 259–271.

Falkowski, Barber & Smetacek (1998). Biogeochemical Controls and Feedbacks on Ocean Primary Production. *Science (New York, N.Y.)*, 281, 200–207.

Falkowski, P.G. (1997). Evolution of the nitrogen cycle and its influence on the biological sequestration of CO2 in the ocean. *Nature*, 387, 272–275.

Field, Behrenfeld, Randerson & Falkowski (1998). Primary production of the biosphere: integrating terrestrial and oceanic components. *Science (New York, N.Y.)*, 281, 237–240.

Finkel, Z.V., Beardall, J., Flynn, K.J., Quigg, A., Rees, T.A.V. & Raven, J.A. (2010). Phytoplankton in a changing world: cell size and elemental stoichiometry. *Journal of Plankton Research*, 32, 119–137.

Finkel, Z.V. & Irwin, A.J. (2000). Modeling size-dependent photosynthesis: light absorption and the allometric rule. *Journal of theoretical biology*, 204, 361–369.

Fox, J. & Weisberg, S. (2019). *An R companion to applied regression.* SAGE, Los Angeles, London.

Geider, R. & La Roche, J. (2002). Redfield revisited: variability of C:N:P in marine microalgae and its biochemical basis. *European Journal of Phycology*, 37, 1–17.

Goldman, J.C., McCarthy, J.J. & Peavey, D.G. (1979). Growth rate influence on the chemical composition of phytoplankton in oceanic waters. *Nature*, 279, 210–215.

Grosse, J., van Breugel, P., Brussaard, C.P.D. & Boschker, H.T.S. (2017). A biosynthesis view on nutrient stress in coastal phytoplankton. *Limnol Oceanogr*, 62, 490–506.

Grover, J.P. (1991). Resource Competition in a Variable Environment: Phytoplankton Growing According to the Variable-Internal-Stores Model. *The American Naturalist*, 138, 811–835.

Guillard, R.R.L. (1975). Culture of Phytoplankton for Feeding Marine Invertebrates. In: *Culture of marine invertebrate animals. [proceedings of the Conference on Culture of Marine Invertebrate Animals, held in Greenport, New York, in October 1972]* (ed. Smith, W.L.). [Springer US], [Boston, MA], pp. 29–60.

Hein, M., Pedersen, M.F. & Sand-Jensen, K. (1995). Size-dependent nitrogen uptake in micro- and macroalgae. *Mar. Ecol. Prog. Ser.*, 118, 247–253.

Hillebrand, H., Acevedo-Trejos, E., Moorthi, S.D., Ryabov, A., Striebel, M. & Thomas, P.K. *et al.* (2022). Cell size as driver and sentinel of phytoplankton community structure and functioning. *Functional Ecology*, 36, 276–293.

Hillebrand, H., Dürselen, C.-D., Kirschtel, D., Pollingher, U. & Zohary, T. (1999). Biovolume calculation for pelagic and benthic microalgae[1]. *Journal of phycology*, 35, 403–424.

Inomura, K., Omta, A.W., Talmy, D., Bragg, J., Deutsch, C. & Follows, M.J. (2020). A Mechanistic Model of Macromolecular Allocation, Elemental Stoichiometry, and Growth Rate in Phytoplankton. *Frontiers in microbiology*, 11, 86.

Irwin, A.J., Finkel, Z.V., Schofield, O.M.E. & Falkowski, P.G. (2006). Scaling-up from nutrient physiology to the size-structure of phytoplankton communities. *Journal of Plankton Research*, 28, 459–471.

Kassambara, A. (2022). *ggpubr: 'ggplot2' Based Publication Ready Plots*.

Kester, D.R., Duedall, I.W., Connors, D.N. & Pytkowicz, R.M. (1967). Preparation of Artificial Seawater. *Limnol Oceanogr*, 12, 176–179.

Kiørboe, T. (1993). Turbulence, Phytoplankton Cell Size, and the Structure of Pelagic Food Webs. In: *Advances in Marine Biology* (ed. Blaxter, J. & Southward, A.J.). Academic Press, pp. 1–72.

Kooistra, W.H. & Medlin, L.K. (1996). Evolution of the diatoms (Bacillariophyta). IV. A reconstruction of their age from small subunit rRNA coding regions and the fossil record. *Molecular phylogenetics and evolution*, 6, 391–407.

Kremp, A., Godhe, A., Egardt, J., Dupont, S., Suikkanen, S. & Casabianca, S. *et al.* (2012). Intraspecific variability in the response of bloom-forming marine microalgae to changed climate conditions. *Ecology and evolution*, 2, 1195–1207.

Legendre, L. & Le Fèvre, J. (1995). Microbial food webs and the export of biogenic carbon in oceans. *Aquat. Microb. Ecol.*, 9, 69–77.

Lenton, T.M. & Watson, A.J. (2000). Redfield revisited: 1. Regulation of nitrate, phosphate, and oxygen in the ocean. *Global Biogeochem. Cycles*, 14, 225–248.

Lewandowska, A.M., Boyce, D.G., Hofmann, M., Matthiessen, B., Sommer, U. & Worm, B. (2014). Effects of sea surface warming on marine plankton. *Ecology letters*, 17, 614–623.

Liefer, J.D., Garg, A., Fyfe, M.H., Irwin, A.J., Benner, I. & Brown, C.M. *et al.* (2019). The Macromolecular Basis of Phytoplankton C:N:P Under Nitrogen Starvation. *Frontiers in microbiology*, 10, 763.

Litchman, E., Edwards, K.F. & Klausmeier, C.A. (2015). Microbial resource utilization traits and trade-offs: implications for community structure, functioning, and biogeochemical impacts at present and in the future. *Frontiers in microbiology*, 6, 254.

Litchman, E. & Klausmeier, C.A. (2008). Trait-Based Community Ecology of Phytoplankton. *Annu. Rev. Ecol. Evol. Syst.*, 39, 615–639.

Litchman, E., Klausmeier, C.A., Schofield, O.M. & Falkowski, P.G. (2007). The role of functional traits and trade-offs in structuring phytoplankton communities: scaling from cellular to ecosystem level. *Ecology letters*, 10, 1170–1181.

Litchman, E., Klausmeier, C.A. & Yoshiyama, K. (2009). Contrasting size evolution in marine and freshwater diatoms. *Proceedings of the National Academy of Sciences of the United States of America*, 106, 2665–2670.

Litchman, E., Tezanos Pinto, P. de, Klausmeier, C.A., Thomas, M.K. & Yoshiyama, K. (2010). Linking traits to species diversity and community structure in phytoplankton. *Hydrobiologia*, 653, 15–28.

Malerba, M.E., Heimann, K. & Connolly, S.R. (2016). Nutrient utilization traits vary systematically with intraspecific cell size plasticity. *Functional Ecology*, 30, 1745–1755.

Malviya, S., Scalco, E., Audic, S., Vincent, F., Veluchamy, A. & Poulain, J. *et al.* (2016). Insights into global diatom distribution and diversity in the world's ocean. *Proceedings of the National Academy of Sciences of the United States of America*, 113, E1516-25.

Marañón, E. (2015). Cell size as a key determinant of phytoplankton metabolism and community structure. *Annual review of marine science*, 7, 241–264.

Marañón, E., Cermeño, P., López-Sandoval, D.C., Rodríguez-Ramos, T., Sobrino, C. & Huete-Ortega, M. *et al.* (2013). Unimodal size scaling of phytoplankton growth and the size dependence of nutrient uptake and use. *Ecology letters*, 16, 371–379.

Mei, Z.P., Finkel, Z.V. & Irwin, A.J. (2011). Phytoplankton growth allometry and size- dependent C:N stoichiometry revealed by a variable quota model. *Mar. Ecol. Prog. Ser.*, 434, 29–43.

Neuwirth & Brewer (2014). *RColorBrewer: ColorBrewer palettes*.

Orizar, I.D.S. & Lewandowska, A.M. (2022). Intraspecific Trait Variability of a Diatom and a Dinoflagellate Along a Salinity Gradient. *Front. Mar. Sci.*, 9.

Pasciak, W.J. & Gavis, J. (1974). Transport limitation of nutrient uptake in phytoplankton1. *Limnol Oceanogr*, 19, 881–888.

Peter, K.H. & Sommer, U. (2012). Phytoplankton cell size: intra- and interspecific effects of warming and grazing. *PloS one*, 7, e49632.

Peter, K.H. & Sommer, U. (2013). Phytoplankton cell size reduction in response to warming mediated by nutrient limitation. *PloS one*, 8, e71528.

Peter, K.H. & Sommer, U. (2015). Interactive effect of warming, nitrogen and phosphorus limitation on phytoplankton cell size. *Ecology and evolution*, 5, 1011–1024.

Peters, R.H. (1993). *The ecological implications of body size.* Univ. Press, Cambridge.

R Development Core Team (2021). *R: A language and environment for statistical computing.,* Vienna, Austria: R Foundation for Statistical Computing.

Raven, J.A. (1994). Why are there no picoplanktonic O 2 evolvers with volumes less than 10 −19 m 3 ? *Journal of Plankton Research*, 16, 565–580.

Raven, J.A. (1998). The twelfth Tansley Lecture. Small is beautiful: the picophytoplankton. *Functional Ecology*, 12, 503–513.

Redfield, A.C., Ketchum, B.H. & Richards, F.A. (1963). The influence of organisms on the composition of sea-water. In: *Hill, M.N. (Ed.) The composition of seawater: Comparative and descriptive oceanography. The sea: ideas and observations on progress in the study of the seas,* pp. 26–77.

Revelle, W. (2022). *psych: Procedures for Psychological, Psychometric, and Personality Research*.

Rynearson, T.A., Richardson, K., Lampitt, R.S., Sieracki, M.E., Poulton, A.J. & Lyngsgaard, M.M. *et al.* (2013). Major contribution of diatom resting spores to vertical flux in the sub-polar North Atlantic. *Deep Sea Research Part I: Oceanographic Research Papers*, 82, 60–71.

Schaum, E., Rost, B., Millar, A.J. & Collins, S. (2013). Variation in plastic responses of a globally distributed picoplankton species to ocean acidification. *Nature Clim Change*, 3, 298–302.

Schulhof, M.A., Shurin, J.B., Declerck, S.A.J. & van de Waal, D.B. (2019). Phytoplankton growth and stoichiometric responses to warming, nutrient addition and grazing depend on lake productivity and cell size. *Global change biology*, 25, 2751–2762.

Siefert, A., Violle, C., Chalmandrier, L., Albert, C.H., Taudiere, A. & Fajardo, A. *et al.* (2015). A global meta-analysis of the relative extent of intraspecific trait variation in plant communities. *Ecology letters*, 18, 1406–1419.

Sommer, U. (1984). The paradox of the plankton: Fluctuations of phosphorus availability maintain diversity of phytoplankton in flow-through cultures1. *Limnol Oceanogr*, 29, 633–636.

Sommer, U., Charalampous, E., Genitsaris, S. & Moustaka-Gouni, M. (2016). Benefits, costs and taxonomic distribution of marine phytoplankton body size. *Journal of Plankton Research*.

Sommer, U., Stibor, H., Katechakis, A., Sommer, F. & Hansen, T. (2002). Pelagic food web configurations at different levels of nutrient richness and their implications for the ratio fish production. *Hydrobiologia*, 484, 11–20.

Sterner, R. & Elser, J.J. (2002). Ecological Stoichiometry: The Biology of Elements From Molecules to The Biosphere, p. 439.

Stolte, W. & Riegman, R. (1995). Effect of phytoplankton cell size on transient-state nitrate and ammonium uptake kinetics. *Microbiology (Reading, England)*, 141, 1221–1229.

Tang, E.P.Y. (1995). The allometry of algal growth rates. *Journal of Plankton Research*, 1325–1335.

Tang, E.P.Y. & Peters, R.H. (1995). The allometry of algal respiration. *Journal of Plankton Research*, 303–315.

Tanioka, T. & Matsumoto, K. (2020). A meta-analysis on environmental drivers of marine phytoplankton C : N : P. *Biogeosciences*, 17, 2939–2954.

Thrane, J.-E., Hessen, D.O. & Andersen, T. (2017). Plasticity in algal stoichiometry: Experimental evidence of a temperature-induced shift in optimal supply N:P ratio. *Limnol Oceanogr*, 62, 1346–1354.

Tréguer, P., Bowler, C., Moriceau, B., Dutkiewicz, S., Gehlen, M. & Aumont, O. *et al.* (2018). Influence of diatom diversity on the ocean biological carbon pump. *Nature Geosci*, 11, 27–37.

Tréguer, P., Nelson, D.M., van Bennekom, A.J., Demaster, D.J., Leynaert, A. & Quéguiner, B. (1995). The silica balance in the world ocean: a reestimate. *Science (New York, N.Y.)*, 268, 375–379.

Tyrrell, T. (1999). The relative influences of nitrogen and phosphorus on oceanic primary production. *Nature*, 400, 525–531.

Valladares, F., Wright, S.J., Lasso, E., Kitajima, K. & Pearcy, R.W. (2000). Plastic Phenotypic Response to Light of 16 Congeneric Shrubs from a Panamanian Rainforest. *Ecology*, 81, 1925–1936.

Violle, C., Enquist, B.J., McGill, B.J., Jiang, L., Albert, C.H. & Hulshof, C. *et al.* (2012). The return of the variance: intraspecific variability in community ecology. *Trends in Ecology & Evolution*, 27, 244–252.

Wickham, H. (2011). plyr: The Split-Apply-Combine Strategy for Data Analysis. *J. Stat. Soft.*, 40, 1–29.

Wickham, H. (2016). *ggplot2. Elegant graphics for data analysis.* 2nd edn. Springer International Publishingr, Cham.

Wickham, H., François, R., Henry, L., Müller, K. & RStudio (2022). *dplyr: A Grammar of Data Manipulation*.

Wickham, H. & Seidel, D. (2022). *scales: Scale Functions for Visualization*.

Winder, M., Reuter, J.E. & Schladow, S.G. (2009). Lake warming favours small-sized planktonic diatom species. *Proceedings. Biological sciences*, 276, 427–435.

# 7|Acknowledgements

First, I like to thank Birte Matthiessen for her supervision, scientific support and encouragement throughout this thesis, and the many fruitful discussions. She always took the time to give guidance and provide helpful comments. I also thank Stefanie Moorthi for her support and supervision, and the opportunity to present my data to a larger group of plankton ecologists. Moreover, I sincerely thank Jorin Hamer for his helping hands during the design, preparation, and conduction of the experiment, as well as for the discussion of the data and the help he provided on the statistical analysis. Thanks also go to Ulrich Sommer, Silvia Pulina, Giannina Hattich, Helmut Hillebrand, and his colleagues in the planktology group at ICBM for further insights and thoughts on stoichiometry in phytoplankton. The technical support of Heike Rickels and Kastriot Qelaj for the chemical analysis of the cellular nutrients and the apprentices Saskia Schlüter, Gideon Jung and Jannis Usinger for their support in the lab is gratefully acknowledged. Finally, many thanks to my friends, family, and especially Sandra Rudeloff for all the support they gave me.

# 8|Appendix

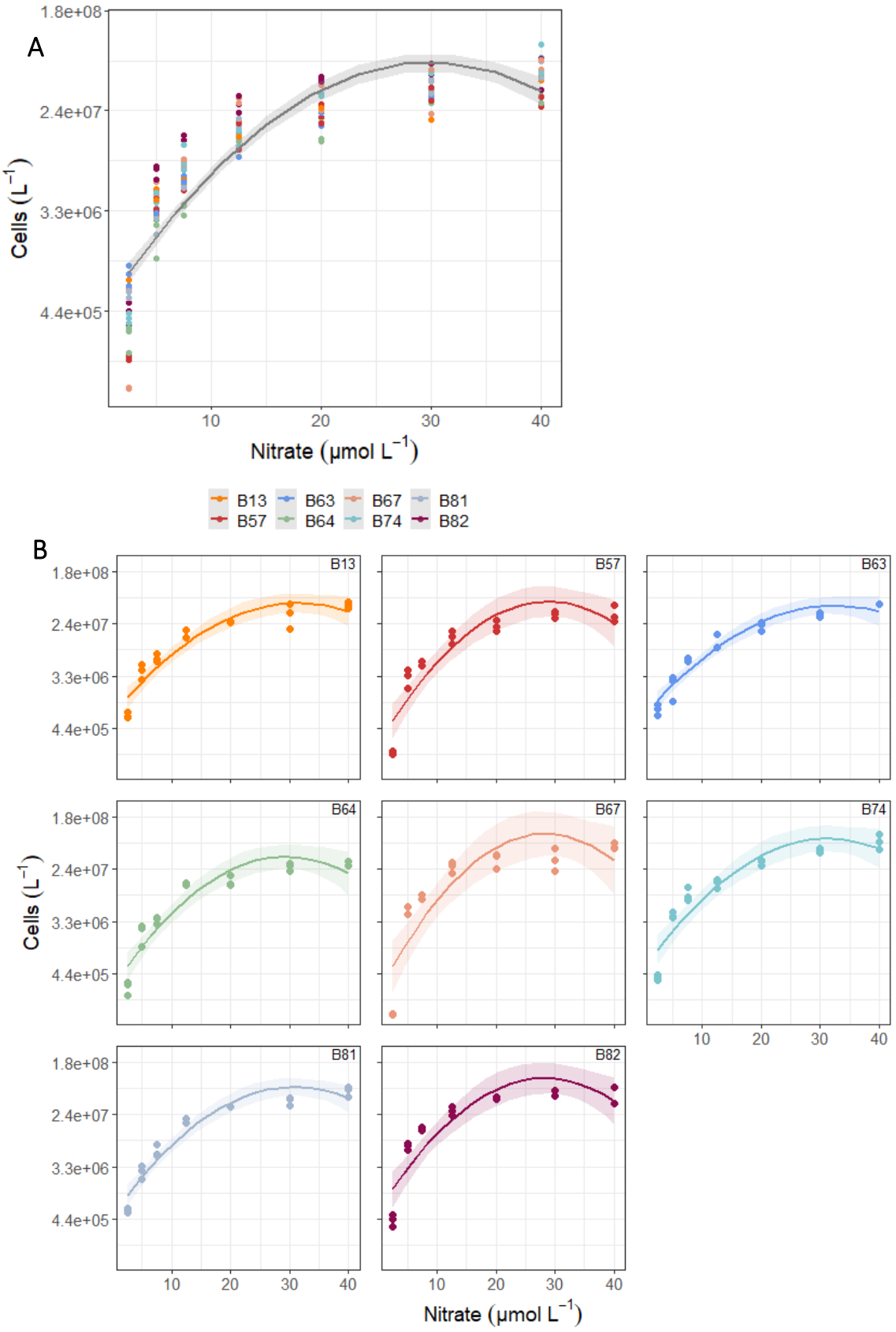


***Figure A 1**: A: Variability among genotypes of cell abundance in cells per liter. B: Plasticity of cell abundance in response to the N treatment of each of the eight genotypes. Colors indicate genotype identity. Line type indicates significance level of the fitted model: solid line ($p \leq 0.05$), dashed line ($0.05 \leq p \geq 0.1$).*

*Table A 1: ANCOVA type III model output of cell abundance in response to the N treatment.*

Cell abundance ($R^2_{adj}$: 0.8315, F= 90.92, p= < 2.2e-16 ***)

```
Anova Table (Type III tests)

Response: ln_Cells_L
                          Sum Sq  Df F value    Pr(>F)
Nitrate_treatment         170.21  1  362.8637 < 2.2e-16 ***
I(Nitrate_treatment^2)    86.34   1  184.0545 < 2.2e-16 ***
Genotype                  10.15   7    3.0926  0.004434 **
---
Signif. codes:  0 ‘***’ 0.001 ‘**’ 0.01 ‘*’ 0.05 ‘.’ 0.1 ‘ ’ 1
```

## Successional stage

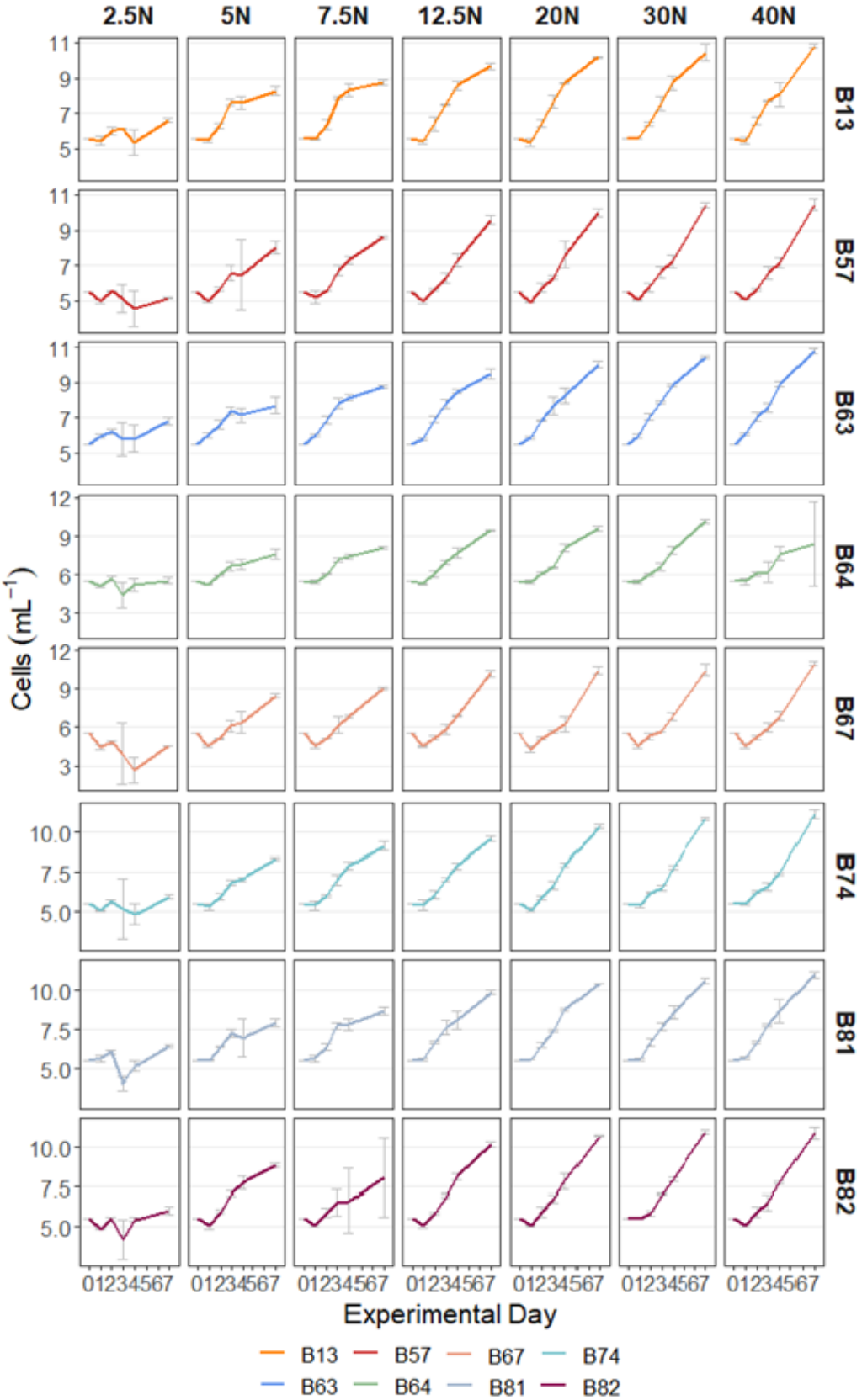


*Figure A 2: Growth curves of the eight genotypes over the course of the experiment (seven days). Mean± SD are shown of log transformed data on cells per milliliter, Y-axis of the genotypes differ. Colors indicate genotype identity.*

## Potential P-limitation

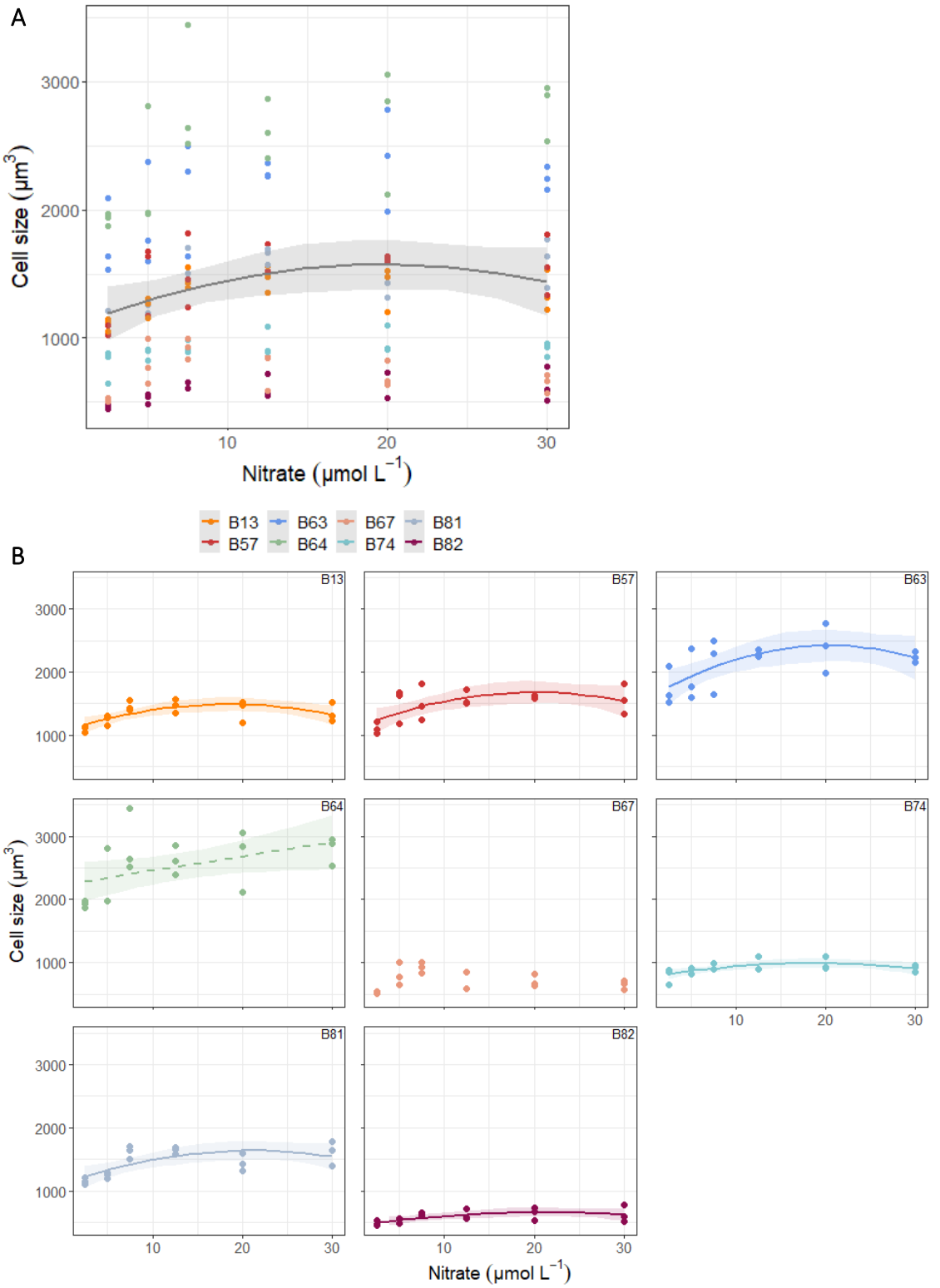


***Figure A 3**: A: Variability among genotypes of cell size. B: Plasticity of cell size in response to the N treatment of each of the eight genotypes, potential P-limited data (40 µmol N $L^{-1}$ treatment) excluded from analysis. Colors indicate genotype identity. Line type indicates significance level of the fitted model: solid line ($p \leq 0.05$), dashed line ($0.05 \leq p \geq 0.1$), no model fitted indicates non-significant.*

*Table A 3: ANCOVA type III model output of cell size in response to the N treatment 40 µmol N $L^{-1}$ treatment excluded from analysis.*

Size ($R^2_{adj}$: 0.8997, F= 80.62, p= < 2.2e-16 ***)

```
Anova Table (Type III tests)

Response: Size_cell_um3
                            Sum Sq  Df F value    Pr(>F)
Nitrate_treatment           1095259 1  23.8824 3.051e-06 ***
I(Nitrate_treatment^2)      1205619 1  26.2888 1.078e-06 ***
Genotype                   14463122 7  45.0532 < 2.2e-16 ***
Nitrate_treatment:Genotype   703783  7   2.1923 0.03915   *
---
Signif. codes:  0 ‘***’ 0.001 ‘**’ 0.01 ‘*’ 0.05 ‘.’ 0.1 ‘ ’ 1
```

*Table A 2: ANCOVA type III model output of cellular nutrients (POC and PON) in response to the N treatment 40 µmol N $L^{-1}$ treatment excluded from analysis.*

POC ($R^2_{adj}$: 0.6284, F= 11.14, p= < 2.2e-16 ***)

```
Anova Table (Type III tests)

Response: ln_Conc_mumol_Cell
                             Sum Sq  Df  F value    Pr(>F)
Nitrate_treatment             1.891   1   5.3342  0.022696 *
I(Nitrate_treatment^2)        1.227   1   3.4608  0.065394 .
Genotype                      6.840   7   2.7558  0.011041 *
Nitrate_treatment:Genotype    8.708   7   3.5082  0.001899 **
I(Nitrate_treatment^2):Genotype   6.814   7   2.7453  0.011314 *
---
Signif. codes:  0 ‘***’ 0.001 ‘**’ 0.01 ‘*’ 0.05 ‘.’ 0.1 ‘ ’ 1
```

PON ($R^2_{adj}$: 0.6671, F= 31.72, p= < 2.2e-16 ***)

```
Anova Table (Type III tests)

Response: ln_Conc_mumol_Cell
                     Sum Sq  Df   F value    Pr(>F)
Nitrate_treatment     60.00   1  172.9013 < 2.2e-16 ***
I(Nitrate_treatment^2)   38.85   1  111.9456 < 2.2e-16 ***
Genotype               7.81   7    3.2153  0.003568 **
---
Signif. codes:  0 ‘***’ 0.001 ‘**’ 0.01 ‘*’ 0.05 ‘.’ 0.1 ‘ ’ 1
```

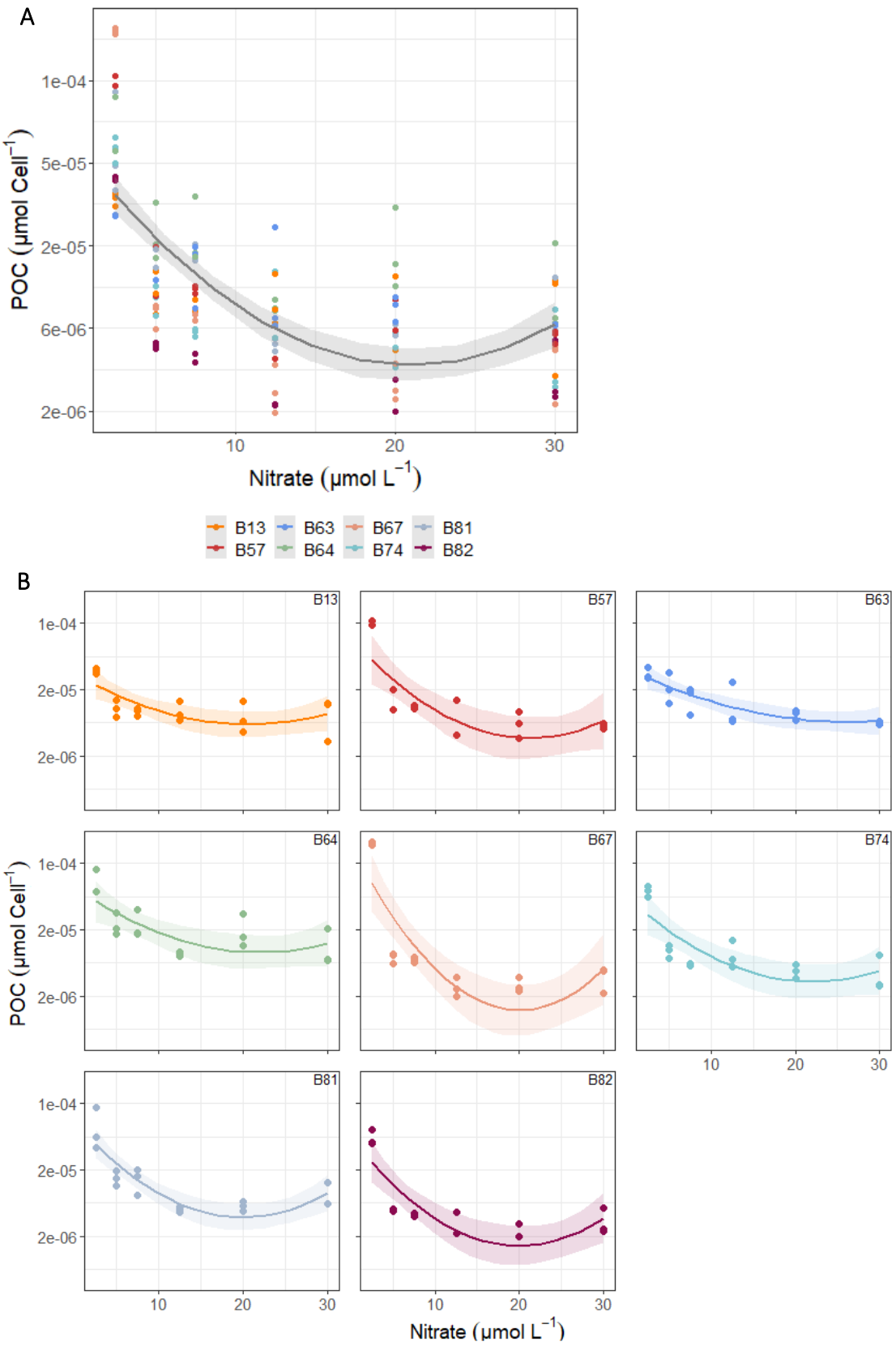


*Figure A 4: A: Variability among genotypes of particulate organic carbon per cell (POC). B: Plasticity of POC per cell in response to the N treatment of eight genotypes, potential p-limited data (40 µmol N L$^{-1}$ treatment) excluded. Line type indicates significance level of the fitted model: solid line ($p \leq 0.05$), dashed line ($0.05 \leq p \geq 0.1$).*

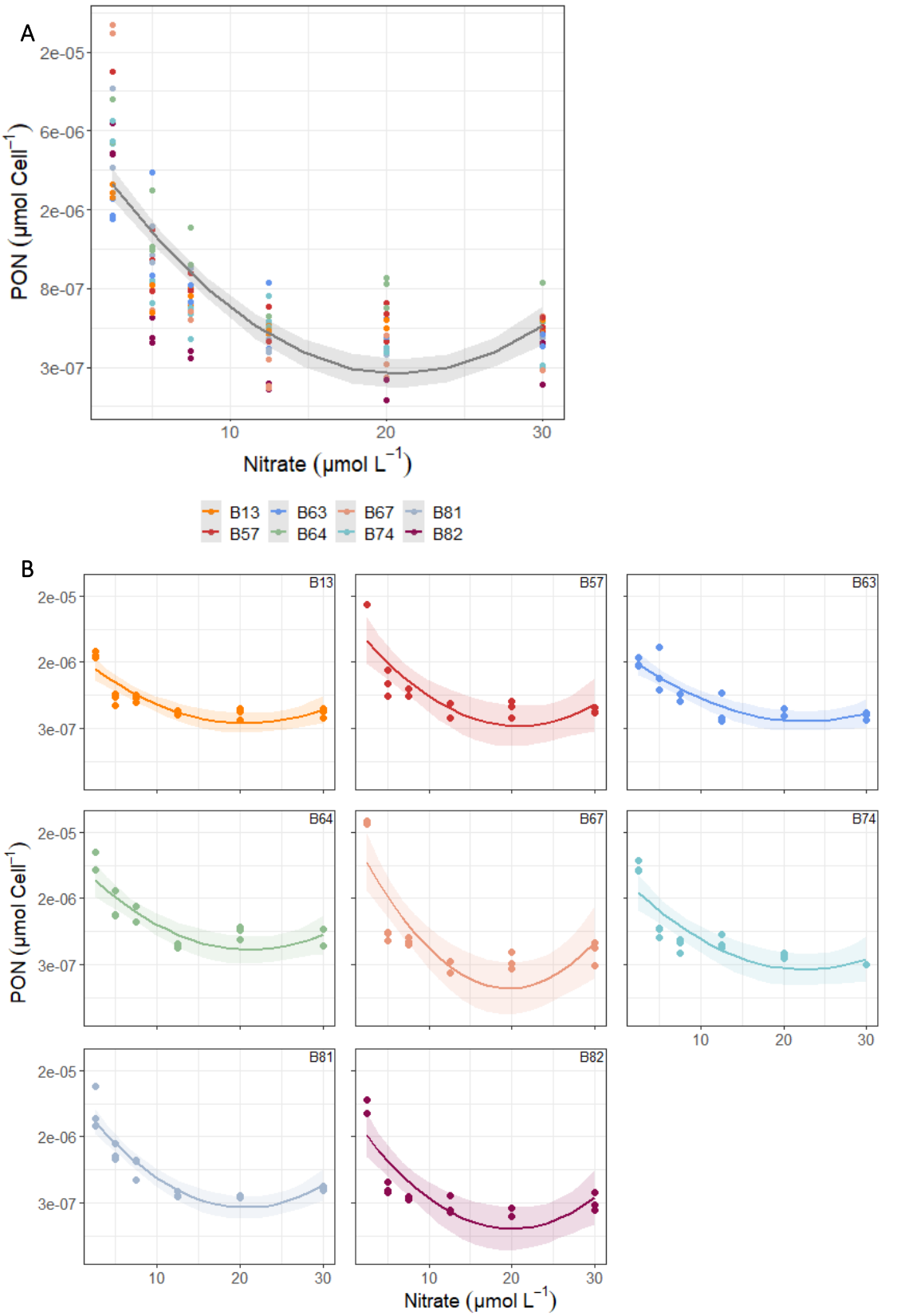


***Figure A 5**: A: Variability among genotypes of particulate organic nitrogen per cell (PON). B: Plasticity of PON per cell in response to the N treatment of eight genotypes, potential P-limited data (40 µmol N $L^{-1}$ treatment) excluded. Line type indicates significance level of the fitted model: solid line ($p \leq 0.05$), dashed line ($0.05 \leq p \geq 0.1$).*

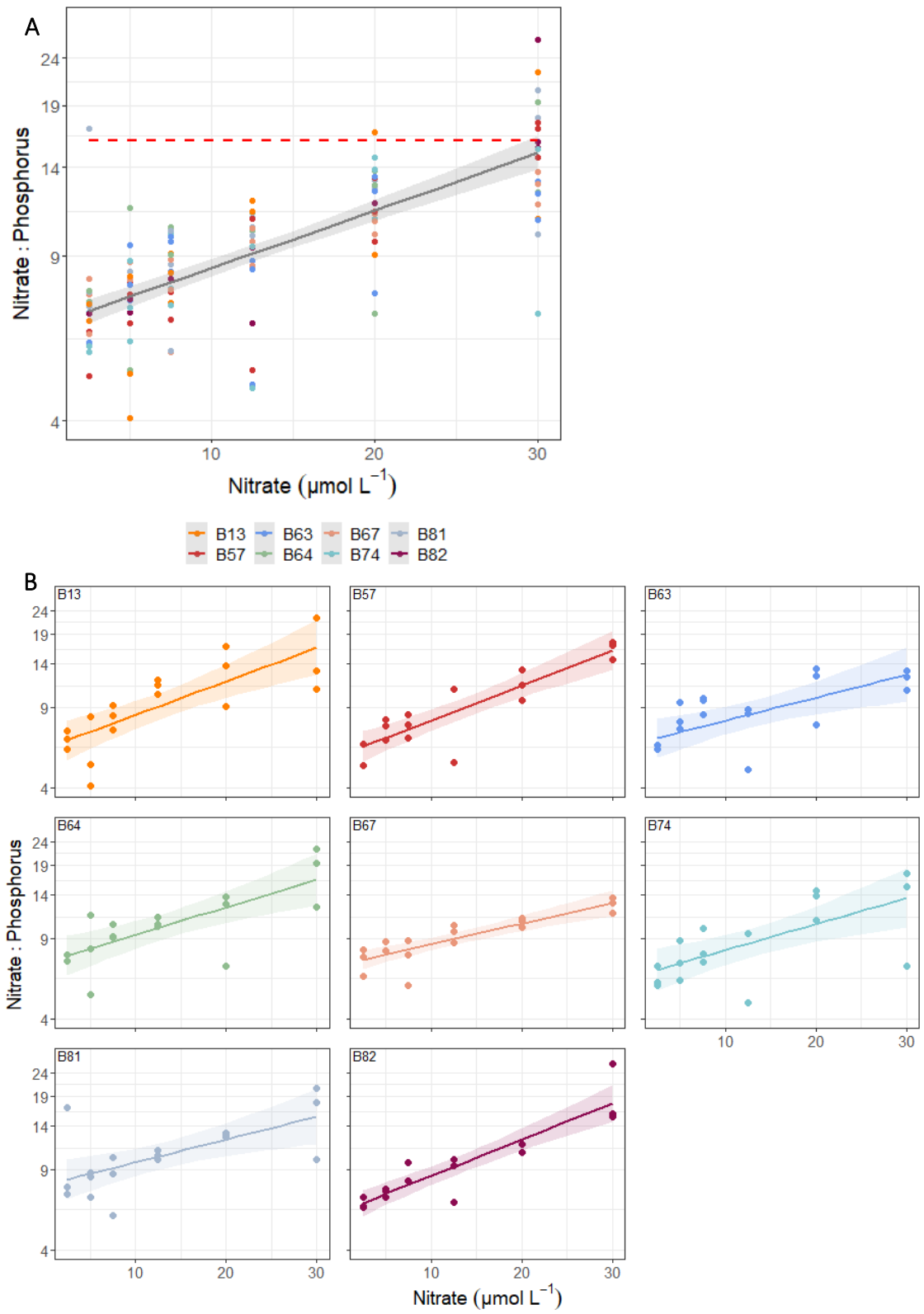


***Figure A 6**: A: Variability among genotypes in Nitrate: Phosphorus (N: P) ratio. B: Plasticity of N: P ratio in response to the N treatment of eight genotypes, potential P-limited data (40 µmol N L$^{-1}$ treatment) excluded. Line type indicates significance level of the fitted model: solid line ($p \leq 0.05$), dashed line ($0.05 \leq p \geq 0.1$).*

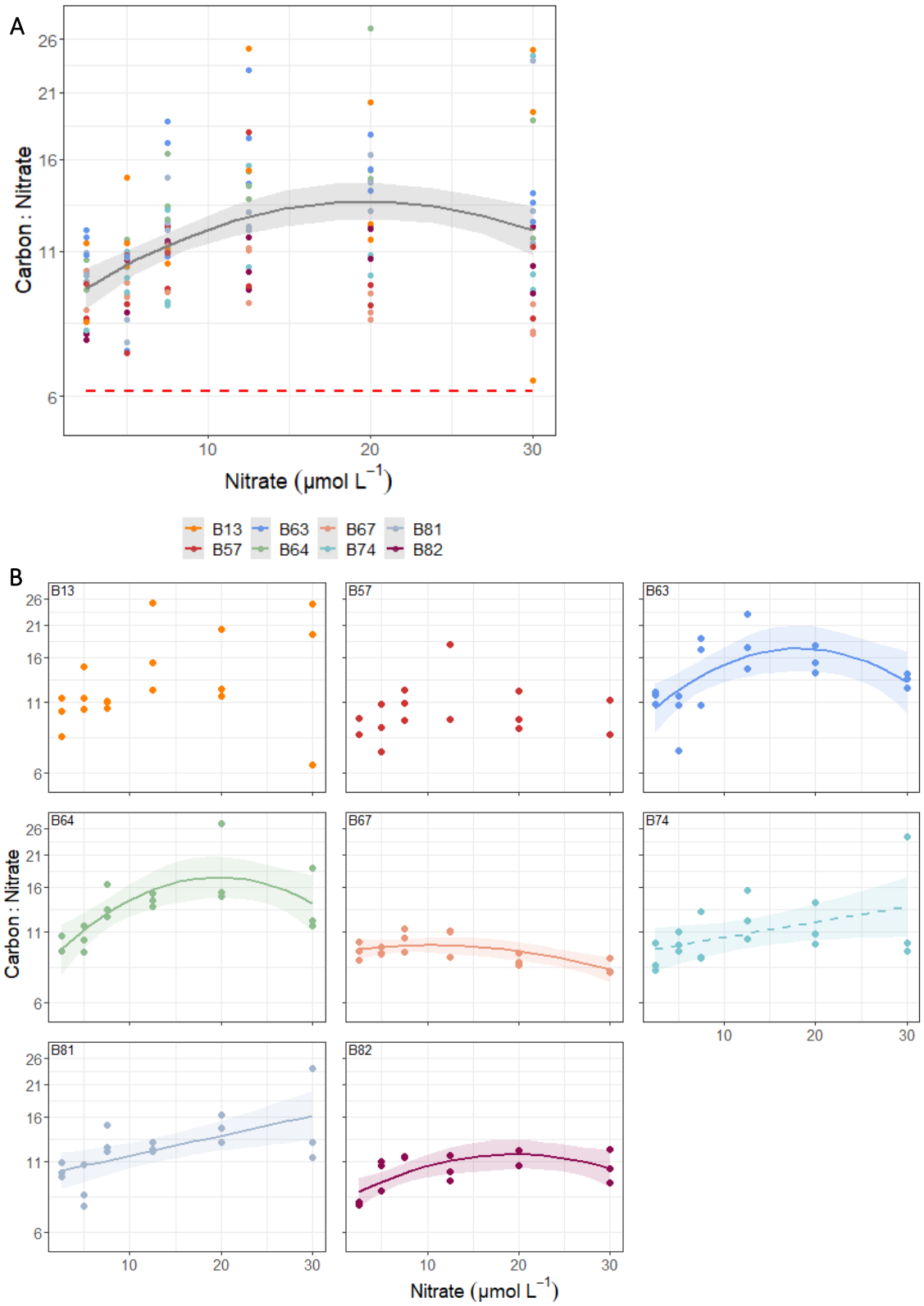


***Figure A 7**: A: Variability among genotypes in Carbon: Nitrate (C: N) ratio. B: Plasticity of C: N ratio in response to the N treatment of eight genotypes, potential P-limited data (40 µmol N L$^{-1}$ treatment) excluded. Line type indicates significance level of the fitted model: solid line ($p \leq 0.05$), dashed line ($0.05 \leq p \geq 0.1$), no model fitted indicates non-significant.*

***Table A 4**: ANCOVA type III model output of cellular stoichiometry (N: P and C: N) in response to the N treatment40 µmol N $L^{-1}$ treatment excluded from analysis.*

NP ($R^2_{adj}$: 0.5727, F= 24.12, p= < 2.2e-16 ***)

```
Anova Table (Type III tests)

Response: ln_Ratio
                    Sum Sq  Df F value    Pr(>F)
Nitrate_treatment   10.284  1  180.5993 < 2.2e-16 ***
Genotype            0.672   7    1.6847 0.1181
---
Signif. codes:  0 ‘***’ 0.001 ‘**’ 0.01 ‘*’ 0.05 ‘.’ 0.1 ‘ ’ 1
```

CN ($R^2_{adj}$: 0.3997, F= 6.743, p= 9.127e-11 ***)

```
Anova Table (Type III tests)

Response: ln_Ratio
                          Sum Sq  Df   F value   Pr(>F)
Nitrate_treatment         1.1383 1   26.2174     1.154e-06 ***
I(Nitrate_treatment^2)    0.8886 1   20.4650     1.419e-05 ***
Genotype                  0.8886 7    1.3218     0.24563
Nitrate_treatment:Genotype  0.5651 7    1.8594     0.08201   .
---
Signif. codes:  0 ‘***’ 0.001 ‘**’ 0.01 ‘*’ 0.05 ‘.’ 0.1 ‘ ’ 1
```

***Table A 5**: Pearson's product-moment correlation output and significance level of cell size and cellular stoichiometry (C:N) of dataset with 40 µmol N $L^{-1}$ treatment excluded.*

| Genotype | C:N [-] |
|---|---|
| B13 | r = 0.4775519, p = 0.051485714 . |
| B57 | r = 0.6320929, p = 0.0137808 * |
| B63 | r = 0.6523309, p = 0.00669 ** |
| B64 | r = 0.5436331, p = 0.032133333 * |
| B67 | r = 0.4232047, p = 0.091577143 . |
| B74 | r = 0.3588227, p = 0.1437 n.s. |
| B81 | r = 0.4288756, p = 0.07575 . |
| B82 | r = 0.7824586, p = 0.0009072 *** |

***Table A 6**: Pearson's product-moment correlation output and significance level of cell size and cellular nutrients (POC and PON) of dataset with 40 µmol N $L^{-1}$ treatment excluded.*

| Genotype | POC [µmol $cell^{-1}$] | PON [µmol $cell^{-1}$] |
|---|---|---|
| B13 | r =-0.490488, p = 0.051693333 . | r =-0.6989004, p = 0.003336 ** |
| B57 | r =-0.533085, p = 0.038262857 * | r =-0.6322986, p = 0.01717 * |
| B63 | r =-0.4071855, p = 0.09352 . | r =-0.5798243, p = 0.018656 * |
| B64 | r =-0.4459408, p = 0.07279 . | r =-0.5710054, p = 0.026656 * |
| B67 | r =-0.4407452, p = 0.08952 . | r =-0.4711461, p = 0.077488 . |
| B74 | r =-0.5584717, p = 0.0256 * | r =-0.603152, p = 0.016106 * |
| B81 | r =-0.6595812, p = 0.005802 ** | r =-0.6938215, p = 0.003744 ** |
| B82 | r =-0.4212533, p = 0.1042 n.s. | r =-0.4842594, p = 0.06552 . |

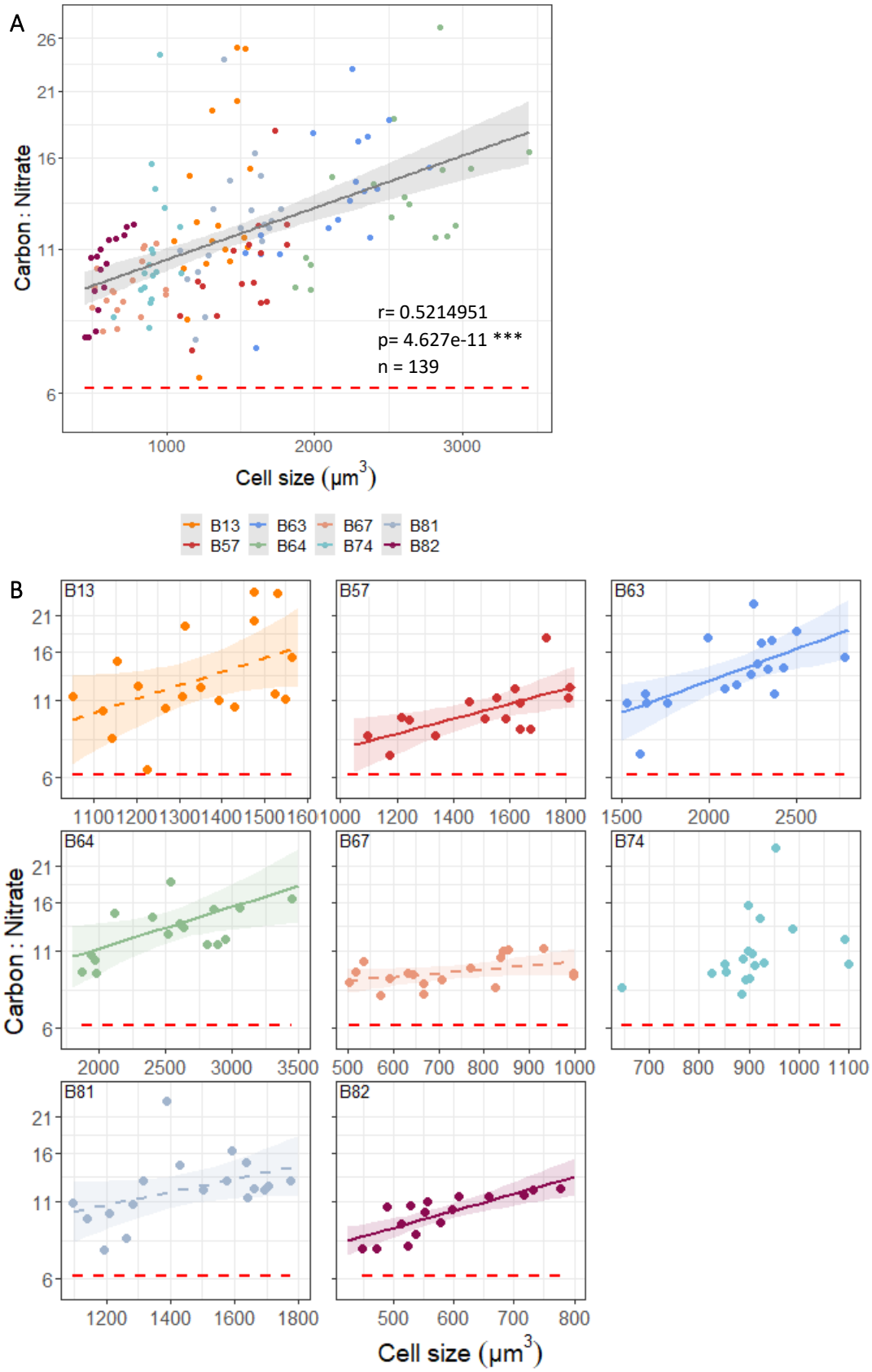


*Figure A 8: Correlation among genotypes of cell size with (A) pooled Carbon: Nitrate ratio, and (B) split by genotype identity, potential P-limited data (40 µmol N $L^{-1}$ treatment) excluded. Colors represent genotype identity. Line type indicates significance level of correlation coefficient: solid line ($p \leq 0.05$), dashed line ($0.05 \leq p \geq 0.1$), no model fitted indicates non-significant. Correlation coefficients see Table A 5.*

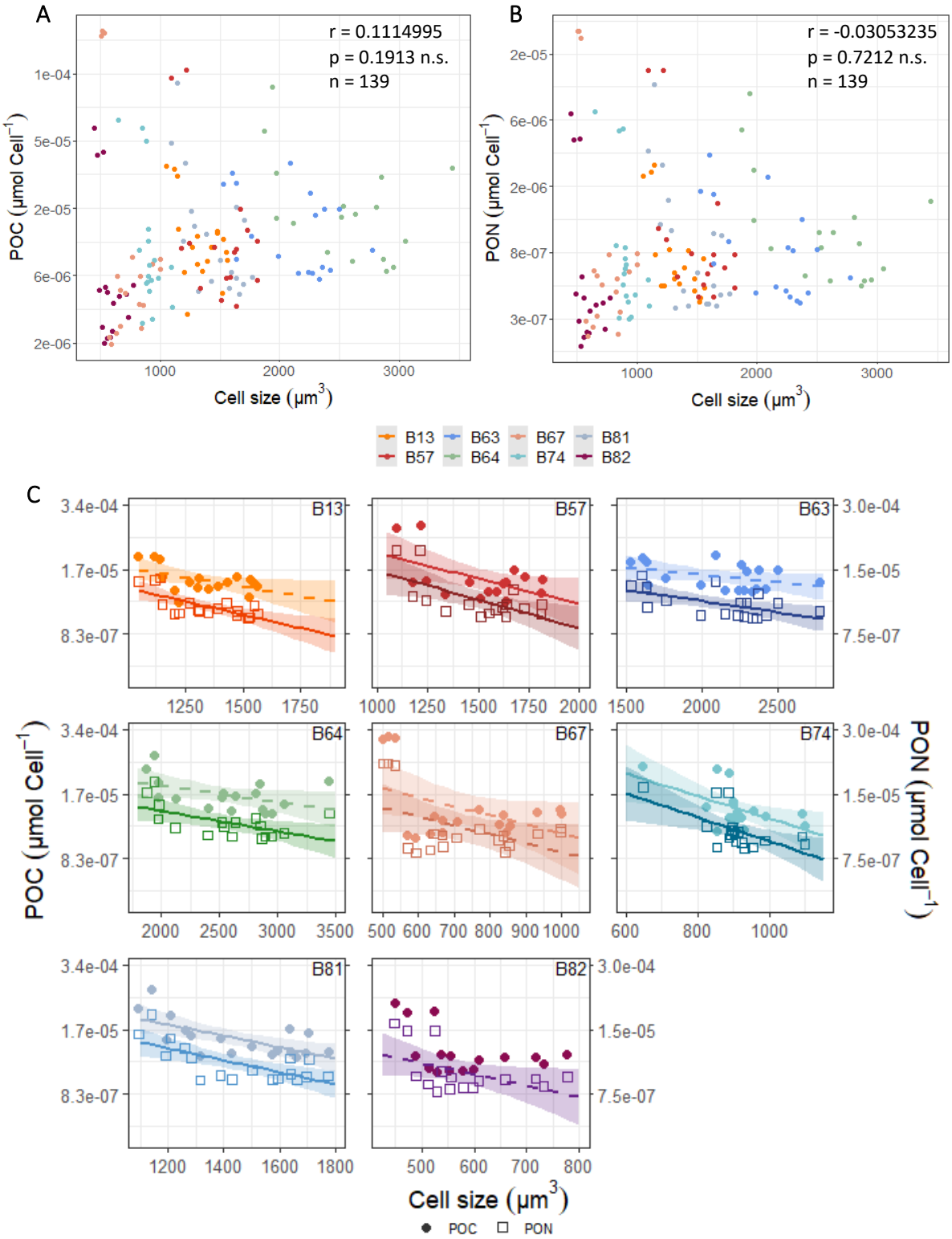


*Figure A 9: Correlation among genotypes of cell size with (A) POC, (B) PON and (C) split by genotype identity. Correlation of cell size and POC (primary y axis, indicated by filled dots) and PON (secondary y axis, indicated by open squares and darker color shade), potential P-limited data (40 µmol N $L^{-1}$ treatment) excluded. Colors represent genotype identity. Line type indicates significance level of correlation coefficient: solid line ($p \leq 0.05$), dashed line ($0.05 \leq p \geq 0.1$), no model fitted indicates non-significant. Correlation coefficients see Table A 6.*

# Declaration of authorship

Hiermit versichere ich an Eides statt, dass ich diese Arbeit selbstständig verfasst und keine anderen als die angegebenen Quellen und Hilfsmittel benutzt habe. Außerdem versichere ich, dass ich die allgemeinen Prinzipien wissenschaftlicher Arbeit und Veröffentlichung, wie sie in den Leitlinien guter wissenschaftlicher Praxis der Carl von Ossietzky Universität Oldenburg festgelegt sind, befolgt habe.

Weiterhin versichere ich, dass diese Arbeit noch nicht als Abschlussarbeit an anderer Stelle vorgelegen hat.

28.10.2022, Julia Romberg